5-2008

Development of Low Temperature Alpha Alumina Coatings by AC Magnetron Sputtering

Andrew Cloud
University of Arkansas, Fayetteville

Recommended Citation

Cloud, Andrew, "Development of Low Temperature Alpha Alumina Coatings by AC Magnetron Sputtering" (2008). *Mechanical Engineering Undergraduate Honors Theses*. 23.
http://scholarworks.uark.edu/meeguht/23

DEVELOPMENT OF LOW TEMPERATURE ALPHA ALUMINA COATINGS BY AC MAGNETRON SPUTTERING

A thesis submitted in partial fulfillment
of the requirements for the Honors Program, for the degree of
Bachelor of Science in Mechanical Engineering

by

Andrew N. Cloud, Mechanical Engineering

Thesis Advisor – Dr. Matthew H. Gordon

May 2007
University of Arkansas

DEDICATION

This work, along with my other accomplishments in the Surface Engineering and Advanced Materials Processing Laboratory, is dedicated to the memory of my former mentor and colleague Dr. Deepak G. Bhat. Dr. Bhat held a Giffels Chair Professorship in the Department of Mechanical Engineering for several years. After accepting an assignment with the National Science Foundation, Dr. Bhat was scheduled to retire from the University of Arkansas in May 2008. However, after a long struggle, Dr. Bhat succumbed to pancreatic cancer last November. His advice and expertise were greatly appreciated, but only fully realized in his absence.

ACKNOWLEDGEMENTS

There are many people I would like to thank for their contributions to my research.

My research adviser, Dr. Matthew Gordon, has been an invaluable asset during the past two years of intensive research. His guidance, advice, and encouragement have contributed greatly to my successes over the past few years.

I would also like to thank Dr. David Glocker and Mark Romach at Isoflux, Inc. Their ICM-10 sputtering system and patient technical support have been much appreciated.

Dr. A.T. Santhanam of Kennametal, Inc., though not directly involved in my work, has been very supportive of the alpha-alumina project at the University of Arkansas.

Dr. Husam H. Abu-Safe has assisted me greatly with the day-to-day lab operations.

Sead Canovic and Dr. Mats Halvarsson at Chalmers University of Technology in Gothenberg, Sweden provided excellent TEM work that added greatly to the understanding of our films.

Dr. Sunil Kumar of the Ian Wark Research Institute, University of South Australia, Dr. Mahendra Kavdia of the Department of Biological Engineering at the University of Arkansas, and Dr. Pravansu Mohanty of the University of Michigan – Dearborn have been vital to understanding how our films perform in a biological environment.

And, finally, I wish to express my gratitude to those students I have worked alongside in the laboratory: Aditya Aryasomayajula, Samuel Mensah, and Sudip Koirala.

TABLE OF CONTENTS

Dedication 1

Acknowledgements 3

Table of Contents 4

Abstract 5

Preface 6

A Brief Introduction 7

Collected Works 9

Contributions to the Included Papers 9

Paper I: "Determining Substrate Temperature in an AC inverted cylindrical magnetron sputtering PVD system"
A.N. Cloud, A. Aryasomayajula, M.H. Gordon, and D.G. Bhat
Surface and Coatings Technology 202 1564-1567 (2008) 10

Paper II: "TEM Investigation of Alpha Alumina Films Deposited at Low Temperature"
A.N. Cloud, S. Canovic, H.H. Abu-Safe, M.H. Gordon, and M. Halvarsson
Submitted to the International Conference on Metallurgical Coatings and Thin Films, Under Review 15

Paper III: "Low Temperature Alpha Alumina Coatings for Biomedical Implant Application"
A.N. Cloud, P. Mohanty, H.H. Abu-Safe, and M.H. Gordon
Submitted to the Society of Vacuum Coaters 36

Paper IV: "Protein Adsorption on Low Temperature Alpha Alumina Films for Surgical Instruments"
A.N. Cloud, S. Kumar, M. Kavdia, H.H. Abu-Safe, and M.H. Gordon
Submitted to the International Conference on Metallurgical Coatings and Thin Films, Under Review 51

Conclusions 69

ABSTRACT

Alpha-phase aluminum oxide thin films were created using an Isoflux ICM-10 dual target inverted cylindrical magnetron sputtering system using mid-frequency AC power supplies. Alpha alumina films were deposited at a magnetron power of 6 kW, 50% oxygen partial pressure by volume, and -35 V DC bias. Film thickness, substrate material, and position and orientation within the deposition chamber were varied.

To ensure the deposition conditions are suitable for alloys, the substrate temperature was measured using temperature indicating liquids. The experimental results, supported by Explicit Euler numerical analysis, revealed a steady state temperature of ~480°C at 6kW.

Transmission electron microscopy (TEM) was used to study alumina films deposited on stainless steel with and without an alpha-phase chromium oxide template layer. The selected area electron diffraction (SAED) patterns indicate that, for both cases, the films tend be predominately alpha-phase with discernable gamma-phase components.

Alpha alumina thin films were deposited on titanium to assess their viability as corrosion and wear resistant biomedical implants. Corrosion resistance tests indicated that the coated titanium had improved performance and stability compared to the uncoated titanium. However, the coefficient of friction increased with the applied film.

Films were deposited on surgical stainless steel substrates to investigate the adsorption of a model protein (BSA, bovine serum albumin). Results indicate that there was a 50% reduction in protein adsorption for samples with the alumina coating compared to those with no coating.

PREFACE

The materials synthesis work presented was conducted in the Surface Engineering and Advanced Materials Laboratory at Engineering Research Center of the University of Arkansas. Data was collected from a variety of labs - identified in the Acknowledgements and papers - between November 2005 and April 2008.

It is the aim of this work to investigate the potential of a unique magnetron sputtering system to deposit alpha-phase aluminum oxide thin films. This material is notoriously difficult to synthesize at temperatures less than 1000°C. The current trend in magnetron sputtering is toward DC, DC pulsed, and HiPIMS (High Power Impulse Magnetron Sputtering) processes. The Isoflux system used utilizes mid-frequency AC power supplies; the results gleaned from the system are inherently different than those obtained by other laboratories. In addition, the inverted cylinder design and unbalanced magnetron create the potential for far higher growth rates than traditional planar magnetron systems. Finally, the size of the ICM-10 system and the capabilities of Isoflux, Inc. make rapid commercialization of any alpha-alumina bearing process relatively straightforward.

This work would not have been possible without the financial support of the National Science Foundation. The research was funded under grants # DMI-0400167 and #0739659.

Andrew N. Cloud

A BRIEF INTRODUCTION

An Isoflux ICM-10 dual target inverted cylindrical unbalanced magnetron sputtering system was used to deposit alpha-phase aluminum oxide coatings on a variety of substrates. Alpha-phase aluminum oxide is a unique material that is of great interest for a number of engineering applications. Alumina may be used in optical coatings, dielectrics, cutting tools, thermal barrier coatings, and biomedical instruments and implants. However, the use of alpha alumina is currently restricted by contemporary deposition methods. Alpha alumina is typically deposited using chemical vapor deposition (CVD) methods where substrate temperatures typically reach 1000°C. While this ensures a good bond between coating and substrate, the thermal expansion mismatch can cause residual stresses to be induced upon cooling. Additionally, the high substrate temperatures preclude the application of the coating to certain temperature-sensitive substrates including polymers and alloys. Physical vapor deposition (PVD) processes have represented a viable alternative to CVD, offering reduced substrate temperatures.

The sputtering system used is a departure from traditional experimental setups. The ICM-10 is considerably more voluminous, allowing large batches of parts to be coated simultaneously. Also, the design exposes a large area of sputter target material to the generated plasma, resulting in a high deposition rate. The unbalanced magnetic field allows ions to migrate to the substrate position near the center of the chamber. This dramatically increases the ion bombardment at the coating. It is this high ion bombardment that is expected to be the mechanism form alpha alumina production at low temperatures.

I believe that it will be possible to form pure alpha-alumina films using this system without that aid of a chromium oxide template layer at 480°C. The importance of this development could not be overstated. The ready availability of a piece of equipment that could perform this feat in a “turn-key” manner would allow the technology to spread rapidly. The estimated market for PVD alpha alumina thin films in the coating industry is ~$400 million. The potential market for biomedical alpha alumina films is expected to be ~$3-5 billion by the end of the decade.

COLLECTED WORKS

Contributions to the Included Papers

The papers presented would not have been possible without the diligent efforts of my collaborators, for whom I am thankful.

In Paper I, “Determining Substrate Temperature in an AC inverted cylindrical magnetron sputtering PVD system,” Aditya Aryasomayajula was responsible for devising a method for measuring the substrate temperatures encountered and procuring the equipment necessary to do so.

Paper II, “Low Temperature Multilayer α-Al_2O_3 Films for Machining Application,” prominently features TEM work performed by Sead Canovic at Chalmers University of Technology in Gothenburg, Sweden.

Paper III, “Low Temperature Alpha Alumina Coatings for Biomedical Implant Application,” focuses on corrosion studies performed at the University of Michigan-Dearborn by Dr. Pravansu Mohanty and his students.

For Paper IV, “Protein Adsorption on Low Temperature Alpha Alumina Films for Surgical Instruments,” I was heavily reliant on Dr. Sunil Kumar of the Ian Wark Research Institute, University of South Australia, Dr. Mahendra Kavdia of the Department of Biological Engineering at the University of Arkansas, and Dan Ostrowski, a graduate student at the University of Arkansas.

Dr. Husam H. Abu-Safe has contributed a great deal to Papers II-IV, specifically by performing materials characterization studies.

Paper I: **“Determining Substrate Temperature in an AC inverted cylindrical magnetron sputtering PVD system”**
A.N. Cloud, A. Aryasomayajula, M.H. Gordon, and D.G. Bhat
***Surface and Coatings Technology* 202 1564-1567 (2008)**

Available online at www.sciencedirect.com

ScienceDirect

Surface & Coatings Technology 202 (2008) 1564 – 1567

SURFACE & COATINGS TECHNOLOGY

www.elsevier.com/locate/surfcoat

Determining substrate temperature in an AC inverted cylindrical magnetron sputtering PVD system

A.N. Cloud [a], A. Aryasomayajula [a], D.G. Bhat [a,b], M.H. Gordon [a,*]

[a] University of Arkansas, Fayetteville, AR 72701, United States
[b] Program Director, SBIR/STTR, National Science Foundation, Arlington, VA, United States

Received 15 June 2007; accepted in revised form 5 July 2007
Available online 31 July 2007

Abstract

The substrate temperature achieved during physical vapor deposition significantly affects the properties and phases of thin films. An Isoflux ICM-10 Dual Target Inverted Cylindrical Magnetron Sputtering system is used to deposit low temperature alpha-phase alumina, for which an experimentally determined substrate temperature is desired. Constraints inherent to the Isoflux system limit the use of a thermocouple. Instead, a pressure vessel containing numerous samples of temperature indicating liquids is placed in the chamber during operation. These indicator paints are observed upon completion of the deposition process to record the substrate temperature. Measurements indicate a temperature range of 343 °C to 399 °C for our alpha-phase alumina films deposited at a pressure of 0.27 Pa (2 mTorr), a substrate bias of −35 V, and a power of 5 kW. Theoretical heat transfer calculations support the experimental measurements. A parametric investigation showed that the removal of the −35 V substrate bias decreases the substrate temperatures by approximately 35 °C and that the substrate temperature increases about 50 °C for each additional kilowatt of power in the range of 1 kW to 6 kW.

Keywords: Substrate temperature measurement; Magnetron sputtering; Alumina films

1. Introduction

Alpha-phase alumina has always been a desirable coating material. It withstands temperatures of 1200 °C, possesses high hardness (24 GPa), and is resistant to corrosion and oxidization [1]. The commercial appeal of alpha-phase alumina films is based in large part on their potential application to high speed steels (HSS) and other cutting tools. However, the deposition of α-Al_2O_3 on steels is limited by the tempering temperature of these substrates.

Alpha alumina has been deposited by CVD [2] and PVD [3–9]. In CVD, the temperature of deposition is roughly 1000 °C, which generally ensures a good metallurgical bond between the substrate and coating. However, the thermal expansion mismatch between carbide substrates and the coating leads to residual tensile stresses that adversely affect adhesion by generating cracks. This process also limits the use of temperature sensitive substrates like HSS; it is therefore desirable to ensure that the substrate does not exceed 550 °C [3]. A suitable alternative to this process is PVD. Using this method, our laboratory has deposited alpha-alumina films at a rate of 330 nm/h, though at an unknown temperature.

While thermocouples are routinely used to monitor substrate temperatures during deposition processes [9–15], technical concerns inherent to the Isoflux ICM-10 Dual Target Inverted Cylindrical Magnetron Sputtering system restrict this method of measurement. Substrate biasing causes an electrical interference between the power supply and thermocouple. While this can be mitigated, the necessary steps add unnecessary cost and complexity to the system. Alternative procedures were investigated, and temperature indicating liquids were selected as the appropriate alternative. In this paper, we will confirm the validity of this method and present results for varying system parameters.

---

[*] Corresponding author.
E-mail address: mhg@uark.edu (M.H. Gordon).

0257-8972/$ - see front matter © 2007 Elsevier B.V. All rights reserved.
doi:10.1016/j.surfcoat.2007.07.007

2. Experimental

Tempilaq G temperature indicating liquids were acquired from Tempil, Inc. of South Plainfield, NJ [16]. The advantages of this product are its ease of application and its direct indication of temperature. The liquids are simply applied by brush to the desired surface where they quickly dry into an opaque film. Once the rated temperature of the paint is reached, it undergoes a distinct phase change that can be observed visually. The use of multiple paints enables one to further discern the temperature. The manufacturer claims an accuracy of ±5 °C.

Selected paints were tested on thin stainless steel test slides in a Lindberg/Blue furnace, model number BF51894C-1. The samples were exposed to temperatures near their rated melting point for 45 min, approximately four times greater than that considered necessary to reach equilibrium. This procedure was then repeated, but this time the paints were applied to the interior wall of the pressure vessel to be used in the Isoflux ICM-10.

Because the ICM-10 and other PVD systems operate at very low pressures on the order of 0.27 Pa (2 mTorr) [17–18], the melting paints and their gaseous emissions pose a potential danger to the internal components of the system. To protect these parts, the paints are contained in a small pressure vessel of AISI 316 stainless steel featuring copper sealant rings. This 13 cm tall pressure vessel is then placed inside the deposition chamber at locations where components to be coated would be placed (Fig. 1). Note that Fig. 1 shows the size of the pressure vessel to scale in relation to the deposition chamber. Multiple temperature indicating liquids, covering a suitable range of temperatures, are painted along the inside wall of the vessel. It is assumed that the presence of the pressure vessel within the deposition chamber has a negligible effect on the working gas and thus the measured temperature.

For the majority of experiments, the pressure vessel was removed and disassembled after 60 minutes of deposition. The temperature indicating paints were observed and assessed for their reaction. Additional repetitions of 15, 45, and 90 min were conducted to verify both steady-state at 60 min, and the accuracy of the theoretical heat transfer model.

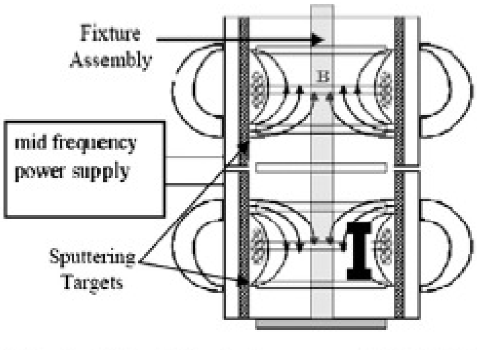

Fig. 1. Experimental schematic showing the pressure vessel inside the ICM-10 chamber (to scale).

Table 1
Properties of AISI 316 stainless steel chamber

Emmisivity	0.57
Density	8000 kg/m^3
Specific heat	500 J/(kg K)
Surface area	2.32×10^{-2} m^2
Volume	1.32×10^{-4} m^3

Multiple substrate biasing (0 V, −35 V, and −88 V) and power conditions (1 kW–6 kW) were imposed on the measurement apparatus. This range of bias and power is commonly used for plasma analysis and thin film deposition.

3. Numerical analysis

The heat transfer during deposition was modeled using numerical analysis methods. The total heat transfer is the sum of two components: radiation from the chamber walls ($\dot{q}_{\mathrm{rad}}$) and ion bombardment ($\dot{q}_{\mathrm{ions}}$). At our low deposition pressure of 0.27 Pa (2 mTorr), the contribution of thermal conduction to the working gas is found to be negligible.

The heat generated by the bombardment of argon ions is assumed to remain constant during the film deposition for a given substrate bias. The heat transfer due to radiation decreases over time as the substrate heats; it is given by Eq. (1)

$$\dot{q}_{\mathrm{rad}} = \varepsilon\sigma A\left(T_S^4 - T_\infty^4\right) \quad (1)$$

where e is the emissivity of the radiating surface, σ is the Stefan–Boltzmann constant, A is the surface area of the pressure vessel, T_S is the substrate temperature, and T_∞ is the temperature of the chamber walls. It should be noted that T_∞ is unknown; the targets of the ICM-10 are water-cooled and their temperature during the deposition process has not been recorded to date.

While the pressure vessel is expected to accumulate an alumina coating during the experiment, we still use the emissivity value for 316 stainless steel in Eq. (1). However, the typical value of both alumina and steel are comparable, and the resulting effect on our model is within the overall uncertainty of our experiment. Thus, our results and conclusions are unaffected by our choice.

The instantaneous change in substrate temperature with respect to time is given by the Eq. (2):

$$\frac{dT_s}{dt} = \frac{-\dot{q}_{\mathrm{ions}} - \dot{q}_{rad}}{\rho V c}, T_S(0) = 20°C = 293\mathrm{K} \quad (2)$$

where, t represents time, ρ represents the density of the steel vessel, V represents the volume of the steel, and c represents the steel's specific heat. Properties for the steel vessel are shown in Table 1 [19–20]. Explicit Euler time integration is used to solve Eq. (2) for substrate temperature as a function of time.

4. Results and discussion

To confirm the accuracy of the thermal indicating liquids, samples were first tested in the controlled conditions of a

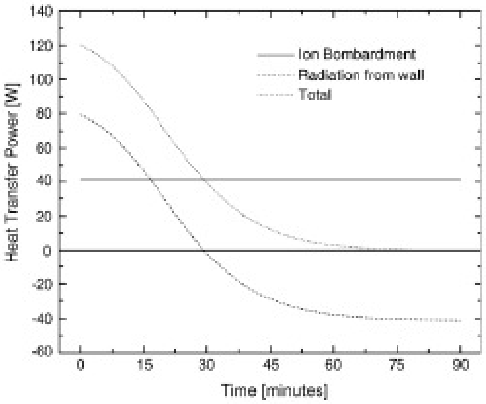

Fig. 2. Heat transfer power components into the pressure vessel as a function of time.

furnace. The Tempilaq G liquids showed significant and consistent phase change within the manufacturer's rated claim of 5 °C. A paint rated for 149 °C, for example, demonstrated obvious melting between 149 °C and 154 °C. This accuracy was determined to be sufficient for the results desired from our deposition experiments. When the furnace testing was repeated using the steel pressure vessel instead of the smaller aluminum slides, the results were the same.

Temperature indicating liquids corresponding to 149 °C, 204 °C, 253 °C, 302 °C, 316 °C, 343 °C, 371 °C, 399 °C, 427 °C, 454 °C, and 510 °C were applied to the interior of the pressure vessel and first tested at a bias of −35 V and a power of 5 kW, conditions known to produce alpha-phase alumina. After 15, 45, 60, and 90 min, the results were observed to compare against our numerical model.

At both the 60 and 90 min increments, the paints corresponding to 253 °C and 302 °C were scorched black, while the paints corresponding to 399 °C and 510 °C were left in their original condition. The paint rated for 343 °C experienced a significant phase change. From this it was concluded that the substrate temperature for this recipe is between 343 °C and 399 °C and that steady state had been attained.

There are two issues that must be addressed to confirm that the temperature measured on the inside of the pressure vessel reflects the substrate temperature of a coated instrument. First, one must prove that the temperatures on the interior of the pressure vessel are indicative of the temperatures on the exterior. However, since no power enters or leaves the center of the chamber, as long as the vessel is in the chamber long enough to reach steady-state, then there will no temperature gradient across the vessel wall. Thus, we need only confirm our second issue, steady-state, to validate our measurements.

Although the measurements at both 60 and 90 min suggest steady state conditions, we also compared these time dependent temperatures against our numerical predictions using Eq. (2). However, to use Eq. (2), we must first specify the chamber wall temperature and the power due to ion bombardment, neither of which are measured in this study. The average ion current density for this system has been estimated by the manufacturer to be 11.3 mA/cm^2 [10]. Therefore, ion bombardment results in a constant input of about 40 W of power to the pressure vessel. The time-dependent radiant heat transfer from the targets depends on the unknown target temperature. Assuming that the indicated temperature range based on the paints represents the correct, steady-state temperature range, the target temperature was chosen such that the predicted steady-state substrate temperature was 371 °C, the middle value of the experimental range for the substrate biased data. At steady state, Eq. (2) indicates that the radiant loss from the vessel to the target wall is equal to the ion bombardment power. Then, using Eq. (1), we can then determine that, to obtain a steady-state vessel temperature of 371 °C, we require a target temperature of 310 °C. The major components of the heat transfer into the pressure vessel and their sum are shown in Fig. 2 (positive powers represent power into the vessel). Initially, the vessel is heated by both ion bombardment and radiation from the walls. Eventually, the vessel becomes hotter than the walls until the net power to the vessel is zero, and steady state is attained.

To check that our assumed chamber wall temperature was reasonable, we next compared the output of the model against our four experimentally obtained temperatures using the paints at 15, 45, 60, and 90 min. Fig. 3 shows both the numerical and experimental data, showing excellent agreement. Note that virtually the same results are obtained for ion bombardment powers between 20 W and 50 W — although the required target temperature must change to again obtain the desired final substrate temperature, the numerical data remain unchanged.

After validating the performance of the paints, we next investigated the effect of both substrate bias (0 V, −35 V, and −88 V) and system power (1 kW–6 kW). The resulting substrate temperatures for these ranges of powers and biases are displayed in Fig. 4. Note that only 1 data point is present at −88 V bias (5 kW power) because this condition damaged our alumina film, and subsequent data at this high bias were not

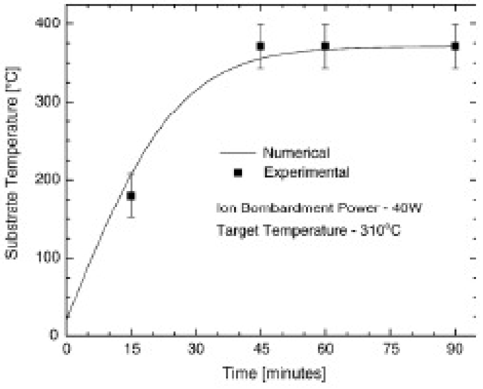

Fig. 3. Numerical and experimental substrate temperature as a function of time for 5 kW system power and −35 V substrate bias.

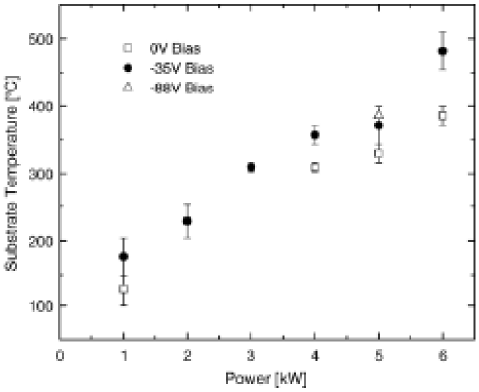

Fig. 4. Substrate temperature as a function of system power and substrate bias.

desired. As expected, the more negatively biased the substrate was, the more ions that were attracted to the substrate and the higher the temperature. Fig. 4 indicates that the application of −35 V increased the substrate temperature by about 35 °C at all powers studied except for 2 kW and 3 kW where the increase was not larger than the sensitivity of the paints. As for the effect of power, the substrate temperature roughly increases by 50 °C for every additional kilowatt of power.

5. Conclusions

Using temperature sensitive paints, the substrate temperatures in a PVD magnetron system were determined as a function of bias and power. The application of a −35 V substrate bias was observed to increase substrate temperatures by approximately 35 °C. Substrate temperatures climbed about 50 °C per each additional kilowatt of power in the range of 1 kW to 6 kW. The temperatures were measured on the interior of a steel pressure vessel after 15, 45, 60, and 90 min of deposition time and numerical simulations confirm that these temperatures represent the true steady-state temperatures, within the accuracy of the paints.

Acknowledgements

The research was supported by the National Science Foundation, under Grant # DMI-0400167.

References

[1] W.H. Gitzen, Alumina as a Ceramic Material, American Ceramic Society, Columbus, 1970.
[2] S. Ruppi, Int. J. Refract. Met. Hard Mater. (2005).
[3] R. Cremer, M. Witthaut, D. Neuschütz, G. Erkens, T. Leyendecker, M. Feldhege, Surf. Coat. Technol. 120-121 (1999) 213.
[4] U. Leushake, T. Krell, U. Schulz, M. Peters, W.A. Kaysser, B.H. Rabin, Surf. Coat. Technol. 94-95 (1997) 131.
[5] M. Mellali, P. Fauchais, A. Grimaud, Surf. Coat. Technol. 81 (1996) 275.
[6] J.R. Sobiecki, J. Ewertowshi, T. Babul, T. Wierzchon, Surf. Coat. Technol. 180-181 (2004) 556.
[7] Y. Chen, X. Ai, C. Huang, B. Wang, Mater. Sci. Eng., A Struct. Mater.: Prop. Microstruct. Process. 288 (2000) 19.
[8] J. Gottmann, E.W. Kreutz, Surf. Coat. Technol. 116-119 (1999) 1189.
[9] T. Kohara, H. Tamagaki, Y. Ikari, H. Fujii, Surf. Coat. Technol. 185 (2004) 166.
[10] A. Belkind, A. Freilich, G. Song, Z. Zhao, R. Scholl, E. Bixon, Surf. Coat. Technol. 174-175 (2003) 88.
[11] O. Zywitzki, G. Hoetzsch, F. Fietzke, K. Goedicke, Surf. Coat. Technol. 82 (1996) 169.
[12] O. Zywitzki, G. Hoetzsch, Surf. Coat. Technol. 86-87 (1996) 640.
[13] O. Zywitzki, G. Hoetzsch, Surf. Coat. Technol. 94-95 (1997) 303.
[14] Jinliu Wang, Yuan-Hsin Yu, S.C. Lee, Yip-Wah Chung, Surf. Coat. Technol. 146-147 (2001) 189.
[15] O. Kyrylov, R. Cremer, D. Neuschütz, Surf. Coat. Technol. 163-164 (2003) 203.
[16] Tempil, Inc. 23 Feb 2007 <http://www.tempil.com/>.
[17] D.A. Glocker, M.M. Romach, V.W. Lindberg, Surf. Coat. Technol. 146-147 (2001) 457.
[18] A. Khanna, D.G. Bhat, Surf. Coat. Technol. 201 (2006) 168.
[19] "Stainless Steel- Grade 316- Properties, Fabrication and Applications." *The A to Z of Materials*. 2007. The A to Z of Materials. 23 Feb 2007 <http://www.azom.com/details.asp?ArticleID=863>.
[20] Transactions in Measurement and Control, 2nd Edition, Omega, vol. 1, 1998, p. 72.

Paper II: **"TEM Investigation of Alpha Alumina Films Deposited at Low Temperature"**
A.N. Cloud, S. Canovic, H.H. Abu-Safe, M.H. Gordon, and M. Halvarsson
Submitted to the International Conference on Metallurgical Coatings and Thin Films, Under Review

TEM Investigation of Alpha Alumina Films Deposited at Low Temperature

A. N. Cloud, University of Arkansas, Fayetteville, AR 72701, USA
S. Canovic, Chalmers University of Technology, Göteborg, Sweden
H. H. Abu-Safe, University of Arkansas, Fayetteville, AR 72701, USA
M. H. Gordon, University of Arkansas, Fayetteville, AR 72701, USA
M. Halvarsson, Chalmers University of Technology, SE-412 96, Göteborg, Sweden

---

Abstract

Alpha-phase aluminum oxide thin films were deposited at 480°C by AC inverted cylindrical magnetron sputtering on nickel coated transmission electron microscopy (TEM) grids and stainless steel substrates. Several previous studies have demonstrated that an alpha phase was possible at low temperature if a chromium template layer was present. However, here we show that alpha phase is possible without the chromium oxide layer. The presence of alpha phase alumina has been confirmed by TEM. Cross-sectional TEM observations have indicated deposition rates as high as 270 nm/h. This intriguing result is attributed to the unique characteristics of the sputtering system which provides more energetic species at the substrate.

I. Introduction

Alpha-phase aluminum oxide coatings have been the subject of great interest over the past thirty years. Alpha alumina is chemically and mechanically stable at temperatures upward of 1000°C and has a melting point of 2053°C [1]. In addition, the alpha-phase exhibits great hardness (24 GPa) and wear resistance [2]. Alpha alumina is widely considered to be the best coating for preventing substrate oxidation at high working temperatures [3]. It is insoluble in inorganic acids and only susceptible to boiling hydrofluoric acid and molten salts at temperatures greater than 1000°C [4].

These exceptional properties make alpha-phase alumina useful for numerous demanding engineering applications. The metalworking industry is constantly seeking a cutting tool to perform at higher cutting speeds in an effort to increase productivity and minimize costs. A cutting tool capable of dry machining would be preferable; the extraneous use of lubricants adds cost and environmentally harmful waste. Due to its stability at elevated temperatures, Al_2O_3 is the ideal coating material for high speed cutting tools. The most desirable form of crystalline alumina coating for cutting tool application is the thermodynamically stable α-phase, commonly known as corundum; this phase has a hexagonal rhombohedral crystal structure.

The formation of these phases is often dependent on the coating technology employed, with substrate temperature being the most influential parameter. An increase in substrate temperature has been correlated to the creation of crystalline phases and the considerable improvement of mechanical and chemical layer properties [5].

Alpha alumina can be deposited by chemical vapor deposition (CVD) [6] and physical vapor deposition (PVD) [7-13]. In CVD processes, the deposition temperature is near 1000°C. This process generally ensures good bonding between the substrate and the grown film, but the thermal expansion mismatch leads to the buildup of residual stress upon cooling that adversely affect adhesion through crack generation. These CVD methods also prohibit the coating of high speed steel (HSS). PVD offers viable alternatives to high temperature deposition. PVD techniques such as e-beam evaporation, pulsed laser deposition, and sputtering have been used to deposit amorphous Al_2O_3 coatings at low temperatures. To obtain an alpha phase, though, the amorphous film is subjected to a temperature of 750°C or more during post-synthesis annealing.

An alternative approach is to grow alumina on an alpha-phase chromium oxide template layer. Alpha alumina and alpha chromium oxide are isostructural [1]. The chromium oxide is considerably easier to form at low temperatures and has only small lattice mismatches with alpha alumina of 4.0% and 4.7% for the *a* and *c* axes, respectively [14]. The ionic radii difference between Al (III) and Cr (III) is approximately 12 % [1]. The two oxides form a system of total solubility [15]. These properties make alpha chromia well-suited as a template layer for the growth of alpha alumina at low temperatures. Following this methodology, Jin *et al.* [16], Morikawa *et al.* [17], Andersson *et al.* [18], and Aryasomayajula *et al.* [19] have reported that alpha alumina could be deposited using a chromium oxide template layer. The lowest temperature for the deposition of alpha-alumina in the literature is 280°C [18], and the maximum deposition rate reported is 150 nm/h [19].

In this paper we report on the deposition of alpha alumina at 480°C [20] without a chromium oxide template layer. A study of alumina films deposited both with and without the template layer shows no significant difference, based on transmission electron microscopy diffraction studies. In all films, the presence of a gamma-phase component increases with film thickness.

II. Experimental

Aluminum oxide thin films of varying thickness and layer configuration were deposited using an Isoflux ICM-10 dual target AC inverted cylindrical unbalanced magnetron sputtering system. As in all sputtering processes, ions in the plasma are directed toward the target wall where they impart enough energy to liberate material from the sputtering targets. High-purity oxygen is metered to the chamber through a mass flow controller and allowed to react with the sputtered metal species to produce the desired oxide coating. Because this system utilizes alternating current, two sputtering targets act as alternating anode and cathode at a frequency of 40 kHz. The aluminum targets are 99.9% pure; chromium targets are also 99.9% pure.

The deposition chamber is approximately 33 cm in diameter and provides roughly 30 cm of deposition space in the vertical direction. The magnetron is powered by an Advanced Energy PE-II AC power supply; substrate biasing is applied by an Advanced Energy MDX DC power supply.

The substrates for these experiments were 316 stainless steel and nickel coated TEM grids. Prior to deposition the substrates were cleaned in an ultrasonic acetone bath for 20 minutes. Samples were then rinsed, dried, and blown free of debris before being placed under vacuum in the chamber. Base pressures of 0.2 mPa were attained. Just before the deposition, substrates were further cleaned by plasma etching using and argon plasma and -80 V of DC biasing.

Films were deposited on 316 stainless steel for periods of 0.5, 1, 2, and 3 hours without a chromia template layer. Additionally, films were deposited for 6 hours on a chromia layer of approximately 200 nm thickness. To avoid a decrease in deposition rate during the 6 hour experiment, targets were de-poisoned after every hour of deposition *in situ*. A mechanical shutter was raised to place a barrier between the substrates and the target. Then, an argon plasma was used to sputter away the insulating layer of aluminum oxide that develops on the target. This process was carried out for 300 seconds; the shutter was then lowered and gas flow rates suitable for deposition were re-established to continue deposition. The deposition pressure was 0.27 Pa. Magnetron power was maintained at 6 kW with an Ar/O_2 ratio of 1:1 during the deposition step. Table I shows the complete deposition parameters. In addition, films were grown in a number of orientations with respect to the sputtering targets to assess the effect of location and orientation on deposition rate, film phase, and morphology.

Subsequent to deposition, coated substrates were allowed to cool under vacuum until they reached room temperature. This process avoids a rapid cooling that may induce film cracking.

The films were analyzed by transmission electron microscopy. For samples deposited on stainless steel, a focused ion beam was used to create a cross-section with a thickness of approximately 125 nm. Diffraction patterns were obtained for points both near the substrate and near the surface of the film.

III. Results and Discussion

Results in the literature have suggested that alpha-alumina grown at low temperatures can only be produced with the aid of an isostructural alpha chromia template [16-19]. However, TEM studies of 100 nm-thick films grown on substrates perpendicular to the sputtering target indicated a pure alpha-phase (Figure 1).

To better investigate the need for the template layer, thicker films, both with and without the template layer, were deposited and analyzed with TEM. Figure 2 shows a TEM micrograph of an 800 nm alumina film deposited on stainless steel with no template for 3 hours. The high deposition rate of ~270 nm/h can be explained by the substrate's position within the chamber. The substrate surface was parallel to the sputtering target at a distance of approximately four inches. Previous samples grown perpendicular to the target were limited to 150 nm/h [19]. Figures 3 and 4 are the selected area electron diffraction (SAED) patterns for the film near the stainless steel and several hundred nanometers away, respectively. Note that the films at both locations are mostly alpha-phase with the presence of some gamma, and that the number of diffraction rings corresponding to the gamma phase is increased further away from the steel.

For comparison, alumina was deposited on a chromia template layer. This deposition was for six hours, and, while the substrate was parallel to the target as before, the distance was increased to nine inches. Figures 5 and 6 are the SAED patterns near and far from the chromia layer, respectively. The results here are much the same as for the alumina film without the template layer. The film is predominantly alpha-phase, becoming less pure throughout its thickness. Note that this film, due to the process of repeated target de-poisoning, is effectively a multilayer film. The mechanical shutter used to block the deposition of metallic aluminum during this crucial step is not entirely effective. Very thin layers of this aluminum can be seen deposited throughout the alumina film (Figure 7). Because thick layers of alumina have been observed in the aforementioned samples to degenerate into a more gamma-like film, it is hoped that these aluminum layers would break up that process, resulting in a more consistently alpha-phase film throughout the entirety of its thickness. Figure 7 also shows the presence of a 100 nm thick layer of pure chrome layer. This film is deposited at the beginning of the deposition run as a consequence of the plasma etching step when no oxygen is present. While the deposition rate of this film was greatly decreased by the increased distance between the target and substrate, the phase of the films was not affected. The deposition rate decreases over time due to a target poisoning effect. Each deposition interval between de-poisoning steps was a one hour, but the thickness of latter layers is clearly decreased when compared to the first three. It is apparent that the de-poisoning step used was not sufficiently long to avoid a rate reduction. Again, the film phase appears unaffected; however, it is clear that the morphology of the film is altered. The film is rough and non-uniform, perhaps a consequence of inconsistent ion flux at this location inside the deposition chamber. High magnification cross sectional TEM was used to observe grains between 5 and 10 nm in size.

To our knowledge, this is the first demonstration of PVD alpha alumina without the aid of a template layer. It is theorized that the unique design of the sputtering system used (with an inverted cylindrical configuration and unbalanced magnetic fields) creates a high current density (10-20 mA/cm^2) that, in combination with the higher ion energies due to the negative substrate bias, is sufficient to overcome the energy barriers to the creation of alpha-phase alumina. The unbalanced magnetic fields promote the migration of ions from the sputtering targets to the substrate platform. These migrating ions will also have additional energy due to the negative substrate bias. Thus, high ion bombardment (both density and energy) may be the key to the development of an alpha-phase film. It should also be noted that, while our deposition temperatures (480°C) are low compared to CVD methods (1000°C), they are higher than the previous PVD methods used to deposit alpha phase (200-250°C). This combination of substrate temperature and high ion bombardment (both density and energy) is unique to this magnetron.

As previously mentioned, it appears that the thicker films contain more gamma phase than do the thinner films. In fact, only the 100nm film is purely alpha phase. One possible explanation is the continued heating of the substrate with time. The substrate enters the chamber at room temperature. During deposition, the temperature increases to the steady state value of

480°C. During this increase of temperature, the coefficient of thermal expansion mismatch between the substrate and the deposited film could lead to stress which affects the resulting phase. Alternatively, it is possible that poisoning of the targets is responsible. Recall that with time the aluminum targets become poisoned which reduces the sputtering rate. Thus, the ratio of oxygen to aluminum in the plasma changes, this ratio has been previously shown to affect the phase of the deposited film [19].

IV. Conclusions

TEM Investigations of alumina thin film growth by AC reactive magnetron sputtering have shown that, even without the use of a chromium template layer, a film that is predominately alpha-phase can be deposited at temperatures near 480°C. A 100 nm-thick film was found to be entirely alpha-phase, while thicker films exhibited more gamma-phase constituents, possibly due to the increasing substrate temperature or to the decreasing amount of sputtered aluminum during deposition. The production of alpha-phase alumina without a template is believed to be the first such result of its kind, and was independent of substrate orientation and position within the chamber. In addition, these films are deposited approximately 3 times more quickly than other PVD processes presented in the literature. These films are believed to be well suited to biomedical applications, where chromium oxide is not desired. Additionally, the production of cutting tool coating by PVD could be economized by simplifying the deposition process.

Acknowledgments

This research was funded by a grant from the National Science Foundation, under Grant # DMI-0400167. The authors would like dedicate this work to the memory of our colleague, Dr. Deepak G. Bhat.

References

[1] E. Ryshkewitch and D.W. Richerson, Oxide Ceramics, General Ceramics, Inc., Academic Press, Inc., Orlando, FL, and Haskell, NJ, 1985.

[2] J. Skogsmo, M. Halvarsson, and S. Vuorinen, Surf Coat. Technol., N/55 (1992) 186.

[3] B. Lux, C. Colombier, H. Altena, K. Stjernberg, Thin Solid Films, 138 (1986) 49.

[4] M.V. Swain, Structure and Properties of Ceramics, 1'01. II, Materials, Science and Technology, VCH Publishers, Weinheim, Germany, 1994.

[5] G. Hoetzch, O. Zywitzki, and H. Sahm, Soc. Vac. Coat., 45th Annual Technical Conference Proceedings, (1997) 77.

[6] S.Ruppi, Int. J. of Refractory Metals and Hard Materials, 23 (2005) 306.

[7] U. Leushake, T. Krell, U. Schulz, M. Peters, W.A. Kaysser, and B.H. Rabin, Surf. Coat. Technol., 94-95 (1997) 131.

[8] J. R. Sobiecki, J. Ewertowshi, T. Babul, and T. Wierzchon, Surf. Coat.Technol., 180-181 (2004) 556.

[9] Y. Chen, X. Ai, C. Huang, and B. Wang, Mat. Sci. Engg., A 288 (2000) 19.

[10] J. Gottmann and E.W. Kreutz, Surf. Coat. Technol., 116-119 (1999) 1189.

[11] R. Cremer, M. Witthaut, D. Neuschutz, G. Erkins, T. Leyendecker, and M. Feldhege, Surf. Coat. Technol., 120-121, (1999) 213.

[12] T. Kohara, H. Tamagaki, Y. Ikari, and H. Fujii, Surf. Coat. Technol., 185, (2004), 166.

[13] A. Belkind, A. Freilich, G. Song, Z. Zhao, R. Scholl, and E. Bixon, Surf. Coat. Technol., 174-175, (2003), 88.

[14] P. Jin, G. Xu, M. Tazawa, and K. Yoshimura, J. Vac. Sci. Technol., A 20 (6), Dec. 2002.

[15] E. W. Bunting, Journal Research Natl. Bur. Standards (U.S) 6, 947 (1931).

[16] P. Jin, S. Nakao, S. X. Wang, and L.M. Wang, Appl. Phys. Lett., 82 (7) (2003) 1024.

[17] Y. Morikawa, T. Satou, and H. Fujii, JP-P2002-53946A.

[18] J. M. Andersson, Zs. Czigany, P. Jin, and U. Helmersson, J. Vac. Sci. Technol. A 22, 117 (2004) 8.

[19] A. Aryasomayajula, S. Canovic, D. Bhat, M.H. Gordon, and M. Halvarsson, Thin Solid Films, v516 (2007) 397.

[20] A. N. Cloud, A. Aryasomayajula, D. G. Bhat, and M. H. Gordon, Surf. Coat. Technol., v202 (2008) 1564.

Table 1 - Deposition parameters for chromium oxide and aluminum oxide coatings.

Parameter	**Chromium Oxide**	**Aluminum Oxide**
Ar/O_2 Ratio	1:1	1:1
Substrate Biasing (V)	-35	**-** 35
Magnetron Power (W)	6000	6000
Base Pressure (mPa)	0.2	0.2
Deposition Pressure (Pa)	0.27	0.27

List of Figures

Figure 1: TEM selected area electron diffraction for a 100 nm alumina film on nickel-coated carbon TEM grid. This film is purely alpha-phase alumina.

Figure 2: TEM micrograph of an 800 nm alumina film deposited directly on 316 stainless steel with no chromium layer. The deposition rate is nearly 270 nm/h.

Figure 3: SAED pattern from 800 nm alumina acquired in the inner part of the layer.

Figure 4: SAED pattern from 800 nm alumina acquired in the outer part of the layer.

Figure 5: SAED pattern from alumina on chromia acquired in the inner part of the alumina layer.

Figure 6: SAED pattern from alumina on chromia acquired in the outer part of the alumina layer.

Figure 7: Cross sectional TEM micrograph of a layered alumina film on a chromia template.

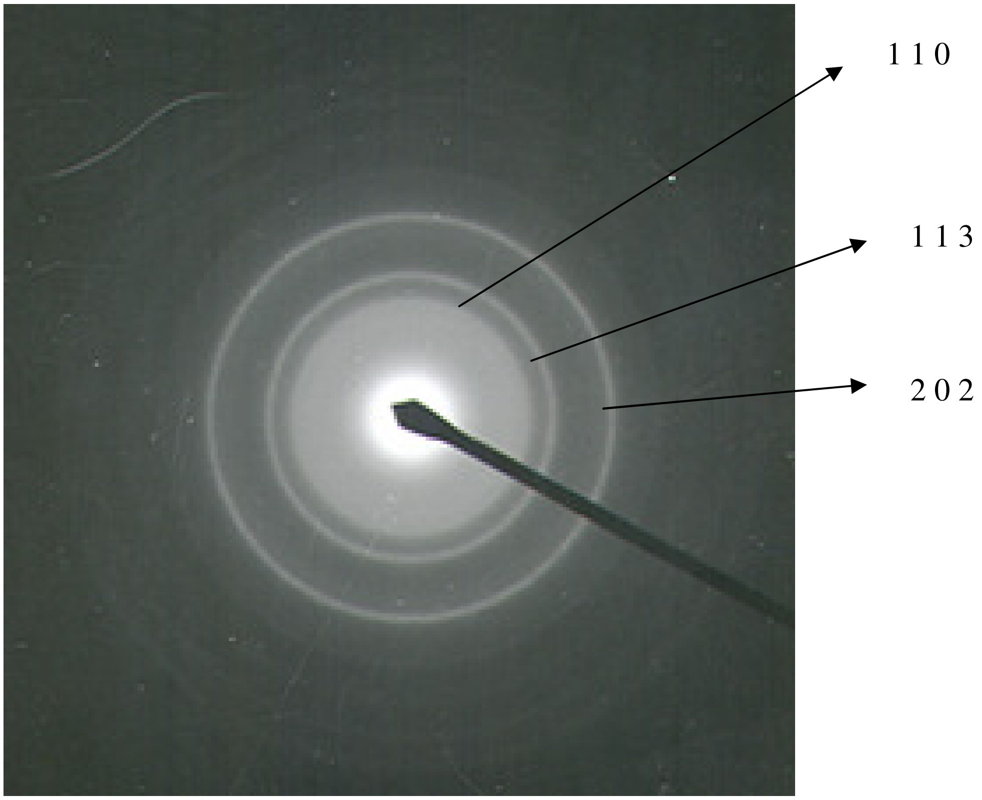

1

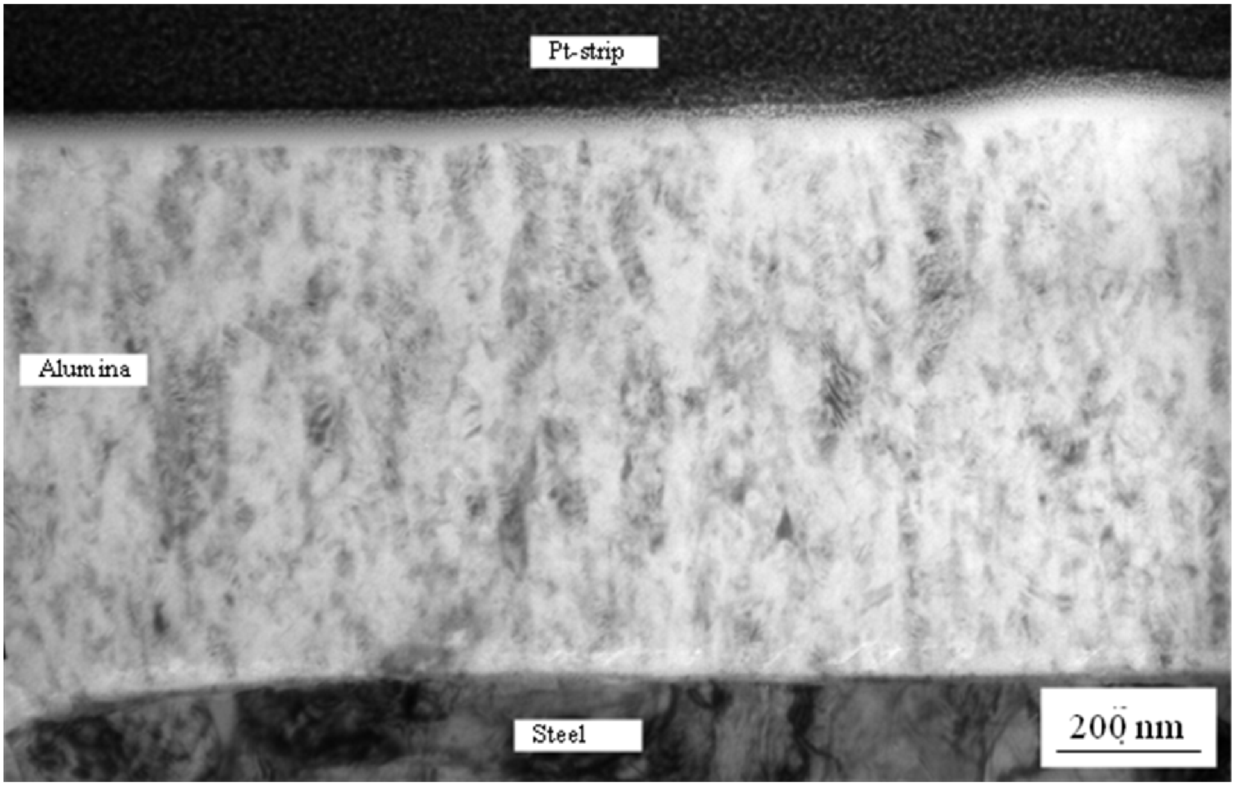

2

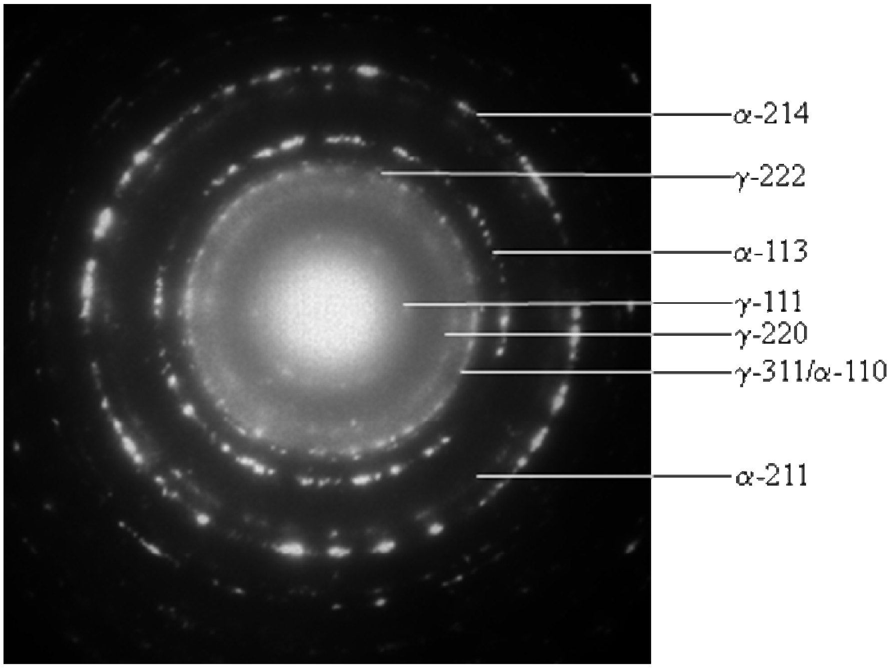

3

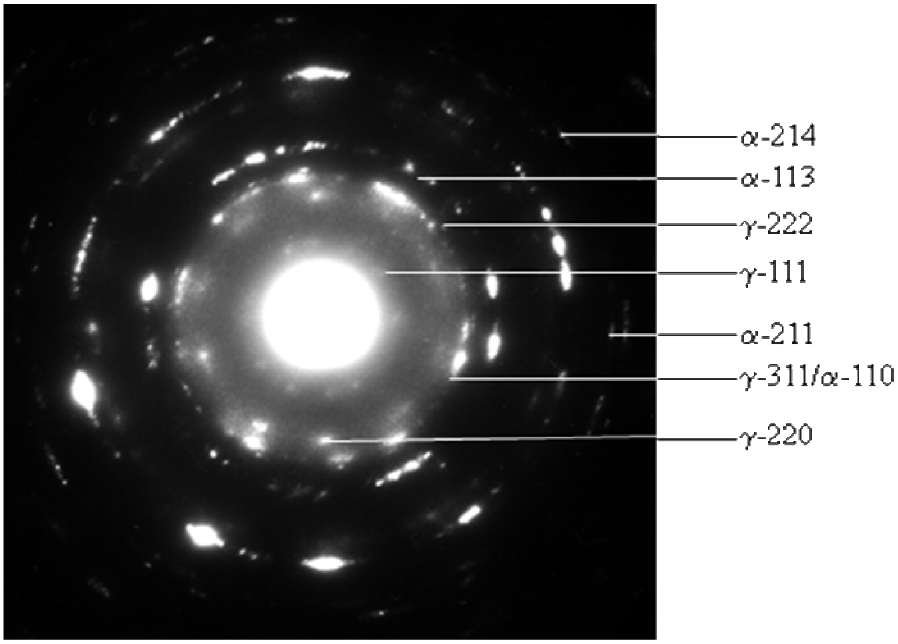

4

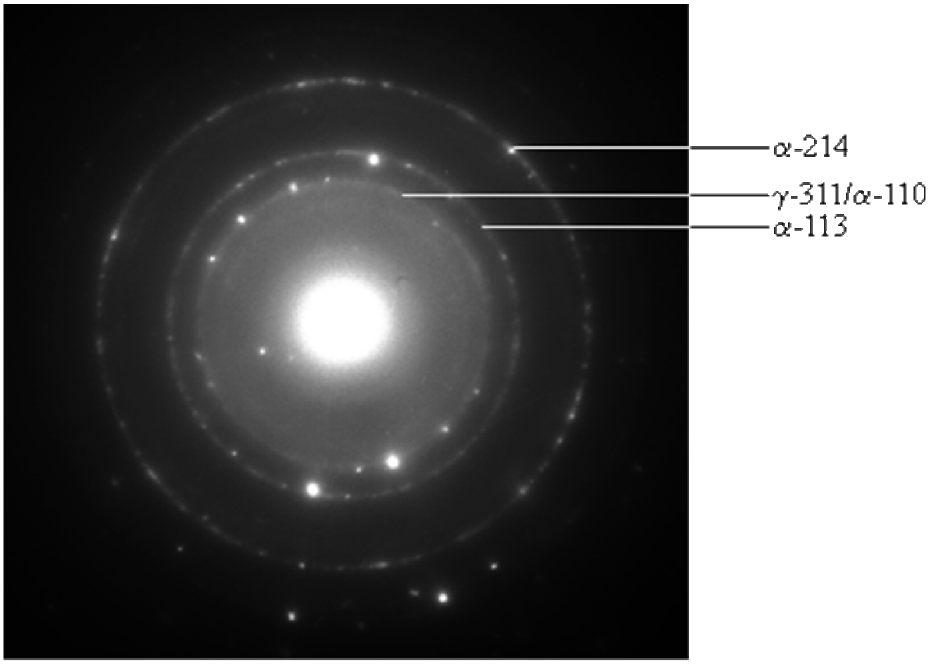

5

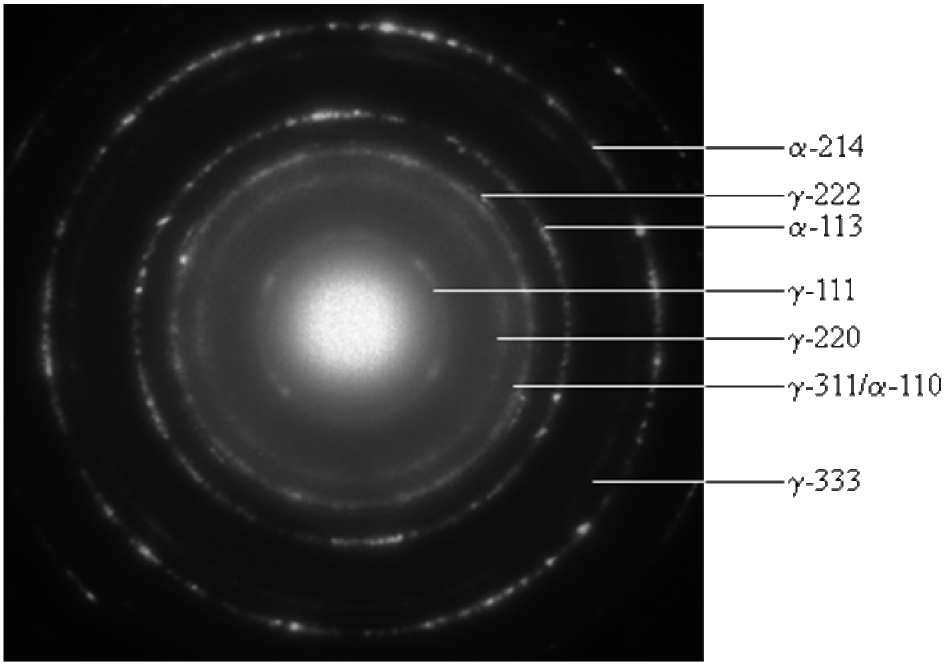

6

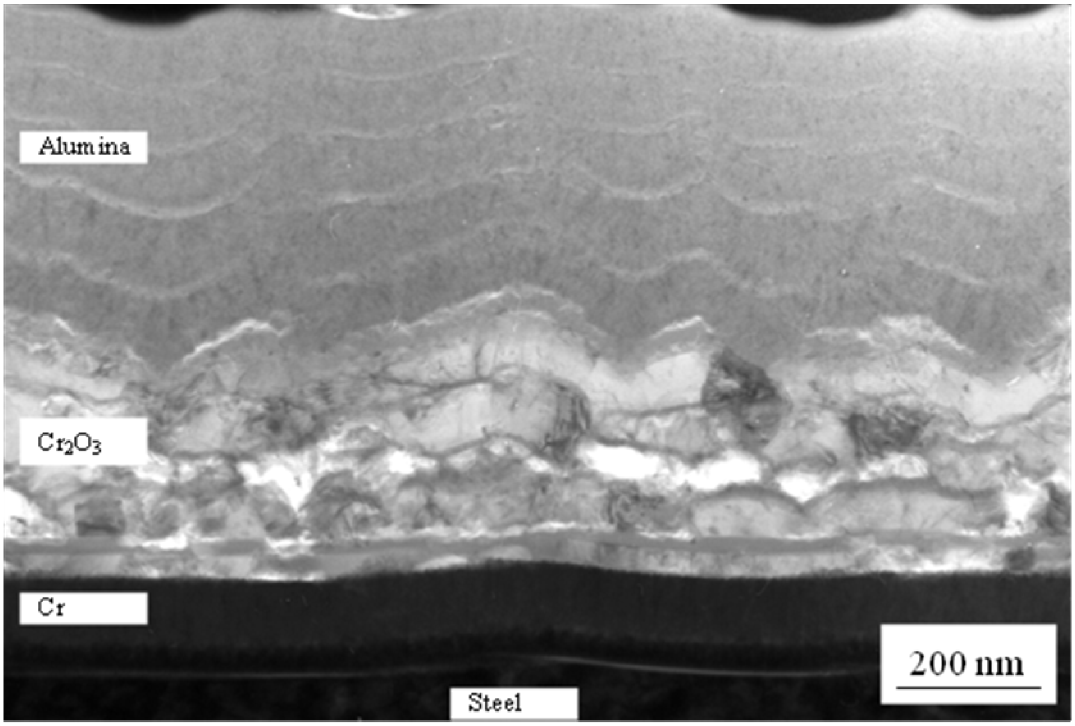

7

Paper III: **“Low Temperature Alpha Alumina Coatings for Biomedical Implant Application”**
A.N. Cloud, P. Mohanty, H.H. Abu-Safe, and M.H. Gordon
Submitted to the Society of Vacuum Coaters

Low Temperature Alpha Alumina Coatings for Biomedical Implant Application

A. N. Cloud, University of Arkansas, Fayetteville, AR 72701, USA
P. Mohanty, University of Michigan - Dearborn, Dearborn, MI 48128, USA
H. H. Abu-Safe, University of Arkansas, Fayetteville, AR 72701, USA
M. H. Gordon, University of Arkansas, Fayetteville, AR 72701, USA

Abstract

Alpha alumina thin films were deposited on titanium to assess their viability as corrosion and wear resistant biomedical implants. The films were deposited at 480°C by AC inverted cylindrical magnetron sputtering technique. No substrate heating (neither before, during, or after deposition) was used. Films were obtained at 6 kW and a 50% oxygen partial pressure by volume. The alpha phase was determined by transmission electron microscopy. Corrosion resistance tests indicated that the coated titanium had improved performance and stability compared to the uncoated titanium. However, the coefficient of friction increased with the applied film.

I. Introduction

Alpha-phase aluminum oxide is well known for its hardness and wear resistance [1]. These properties make alpha-phase alumina useful for several engineering applications requiring a hard coating [2]. These films are employed as coatings for magnetic read-write heads of hard disks [3], cutting tools [2], and a number of other components that will be subjected to great wear. Aluminum oxide exists in an amorphous structure or an array of metastable phases. The thermodynamically stable alpha-phase has a hexagonal rhombohedral crystalline structure and is the most desirable form for many high wear applications.

The deposition of alpha alumina by chemical vapor deposition (CVD) at temperatures near 1000°C has been well established [4]. This process generally ensures a good metallurgical bond between the substrate and the coating, but the thermal expansion mismatch between the two leads to residual stresses that can generate cracking of the film.

Physical vapor deposition, in contrast, is suitable at temperature as low as 280°C [5]. PVD includes electron beam evaporation, plasma spraying, gas detonation, laser ablation, RF sputtering, DC- and pulsed DC magnetron sputtering, and mid-frequency AC magnetron sputtering, each of which has been used to deposit amorphous alumina coatings. For an alpha phase, however, post-deposition heating in excess of 750°C is required, eliminating the low temperature benefit of the PVD process [6-13].

An alternative approach is to promote the growth of alpha alumina using an alpha-phase chromium oxide template layer. Jin *et al.* [14], Morikawa *et al.* [15], Andersson *et al.* [5], and Aryasomayajula *et al.* [16] have reported that alpha alumina can be deposited using a chromium oxide template layer. Because alpha alumina and alpha-phase chromium oxide are isostructural [17], the deposition of alpha-alumina is encouraged by the presence of the chromia layer.

For this application, however, it is desired to have alpha-alumina directly on titanium substrates (no template layer). As detailed here, our preliminary depositions with a template layer have been successful, and the stated advantages of alumina make it an ideal coating for hip and knee replacements. The reduction in wear rates would increase the working lifetime of the implant and thus reduce the likelihood that a replacement procedure would be required during a patient's lifetime. Also, lower wear would translate into a reduction of debris from the implant surfaces. Particles generated by wear of prosthesis surfaces often cause pain and swelling in the surrounding tissue and can eventually lead to loosening of the device [18, 19]. Additionally, $\alpha-Al_2O_3$ is less likely to decompose in the body than the other less stable alumina structures [20]. Finally, it has been reported that ceramic oxides have an advantage over other ceramic coatings for prostheses because the body's natural joint lubricants bond better to surfaces containing oxygen.

II. Experimental

Thin films of aluminum oxide were deposited on medical grade titanium alloy substrates using an Isoflux ICM-10 dual target AC inverted cylindrical unbalanced magnetron sputtering system. In this system, two sputtering targets act as alternating anode and cathode at a frequency of 40 kHz. High-purity gas is supplied to the chamber and allowed to react with the sputtered metal species to form an oxide coating. The plasma is sustained with an argon working gas.

The sputtering chamber is approximately 13 inches in diameter and provides roughly 12 inches of deposition space in the vertical direction. The magnetron is powered by an Advanced Energy PEII alternating current power supply that is operated at 6 kW for this experiment. Voltage biasing of -35 V was supplied by an Advanced Energy MDX DC power supply.

Prior to deposition, the substrates were cleaned in an ultrasonic acetone bath for 20 minutes. Samples were then rinsed, dried, and blown free of dust debris before being placed under vacuum in the chamber. Base pressures of 1.5×10^{-6} Torr were attained. Just before deposition, substrates are further cleaned by plasma etching using an argon plasma and -80 V of DC biasing. Chromium rings of 99.9% purity were sputtered for 15 minutes at 6 kW with an Ar/O_2 ratio of 1:1 to create a Cr_2O_3 template layer. The deposition chamber was then vented and aluminum sputtering targets (99.99% pure) were installed. Once the desired base pressure was attained again, aluminum oxide was deposited for a period of 6 hours. The deposition pressure was 2 mTorr. Substrate temperatures during deposition have been shown to be approximately 480°C [21]. Subsequent to deposition, coated substrates were allowed to cool under vacuum to avoid film cracking. This coating has been observed to be approximately 750 nm thick in total. The films were analyzed by TEM for phase analysis. The wear behavior was studied using a pin-on-disc type tribometer to obtain the coefficient of friction.

The corrosion behavior of the coatings was studied by electrochemical methods. A Princeton Applied Research (PAR) flat cell (Figure 1) was used. The electrolyte, a Hank's solution, is a simulated body fluid and was obtained from Mediatech, Inc. Potentiodynamic scans and electrochemical impedance spectra (EIS) were determined using the Solartron multistat and a frequency analyzer. Prior to the polarization scan the samples were kept in solution to establish the free corrosion potential (Ecorr). Electrochemical impedance experiments were performed at the open circuit potential. Subsequently, the potentiodynamic polarization curves were obtained with a scan rate of 1mV/s.

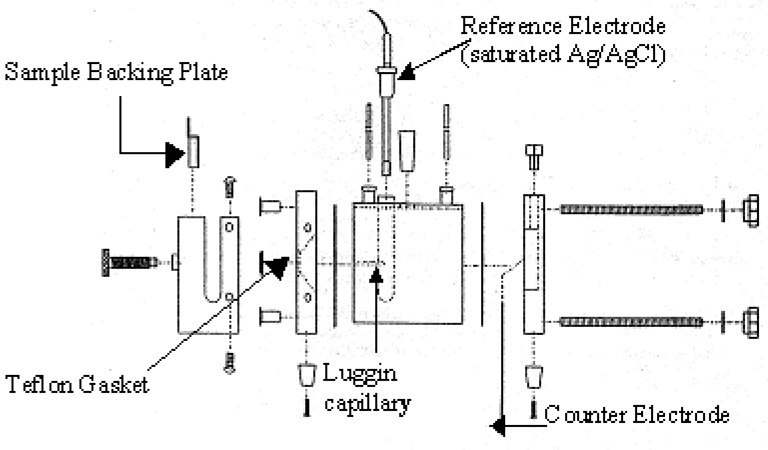

Figure 1: **Flat corrosion cell used for corrosion study (Princeton Applied Research).**

III. Results and Discussion

Transmission electron microscopy has been used in the past to determine the phase of this film. This TEM work confirms that, near the chromia pre-coat, the alumina is alpha-phase [16]. In other work, we confirmed a pure alpha phase for alumina directly on a nickel TEM grid, although the film was only 80 nm thick.

The polarization curves on bare titanium and the alumina-coated titanium are shown in Figures 2 and 3. These scans were repeated 3 times in each case. From the inspection of the polarization curves, the onset of passivity in the case of bare titanium occurs at higher potential compared to that of the coated sample. The passivity in titanium occurs due to oxide formation. In the case of the coated samples, the presence of the alumina film shows a passive behavior at lower potentials. At higher potentials the coated sample appears to develop pitting. However, SEM examination of sample did not reveal any pits; the film was very stable without any indication of dissolution.

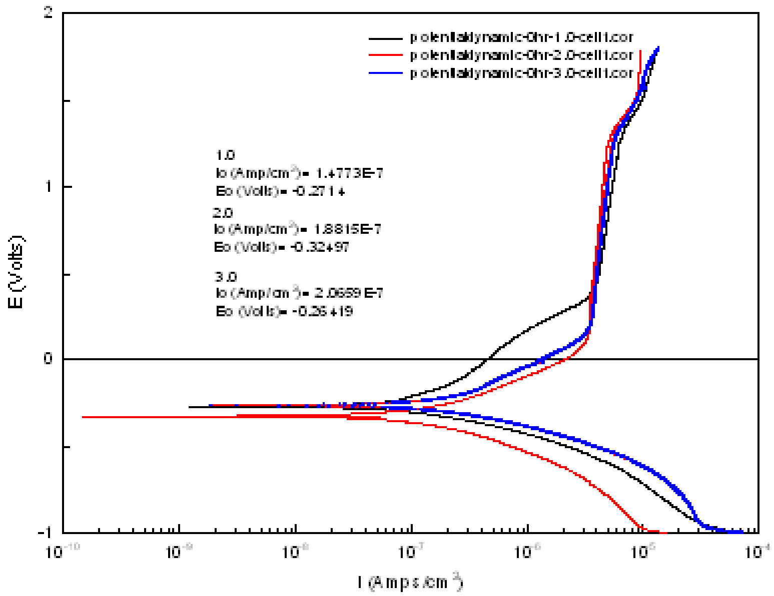

Figure 2: **Polarization curves measured on bare titanium surface.**

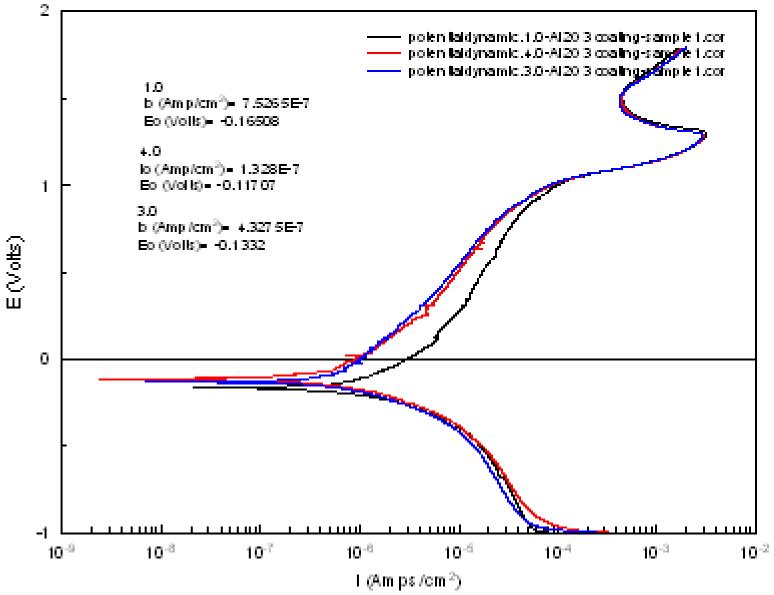

Figure 3: **Polarization curves measured on alpha-alumina coated titanium surface.**

Electrochemical impedance experiments were performed at the open circuit potential. The impedance spectra obtained at different exposure times during the immersion in Hank's simulated body fluid are shown in Figures 4, 5 and 6. They are displayed in both complex impedance (Nyquist diagram) and Bode amplitude and phase angle plots. The Nyquist plots are relatively featureless, but the Bode plots indicate changes in the electrochemical characteristics of the system with time. It was observed that upon immersion of the uncoated specimen in the electrolyte, variations in the impedance spectra occurred with exposure time, which resulted from the evolution of the film on the bare titanium sample. Changes are not noticeable for coated samples with time elapsing. Even after 158 hours of exposure, an almost stationary behavior was reached. These observations clearly show that the alumina coating is very stable and provide the desired corrosion resistance.

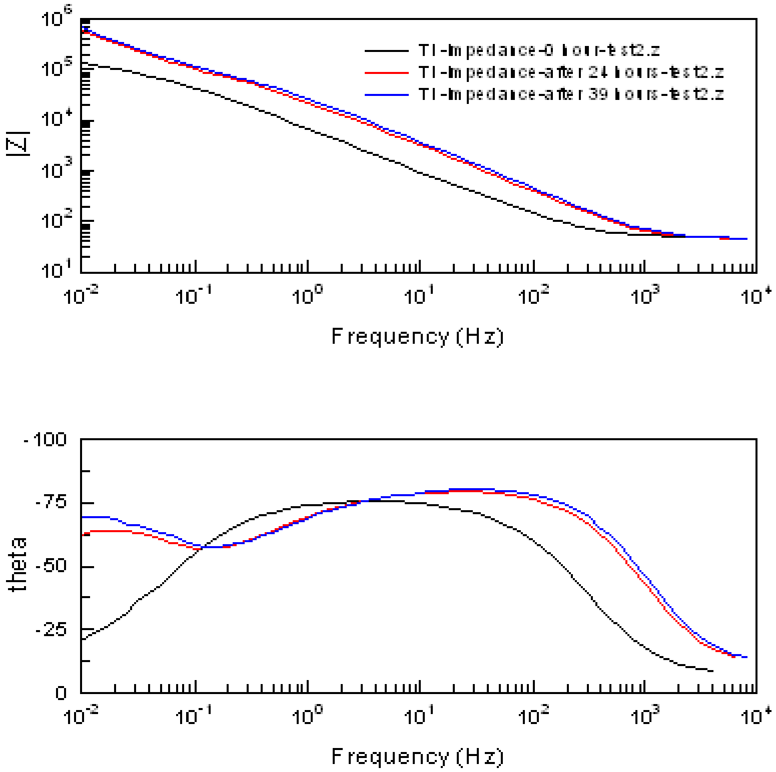

Figure 4: **Impedance spectra recorded for Ti in Hank's solution at various times.**

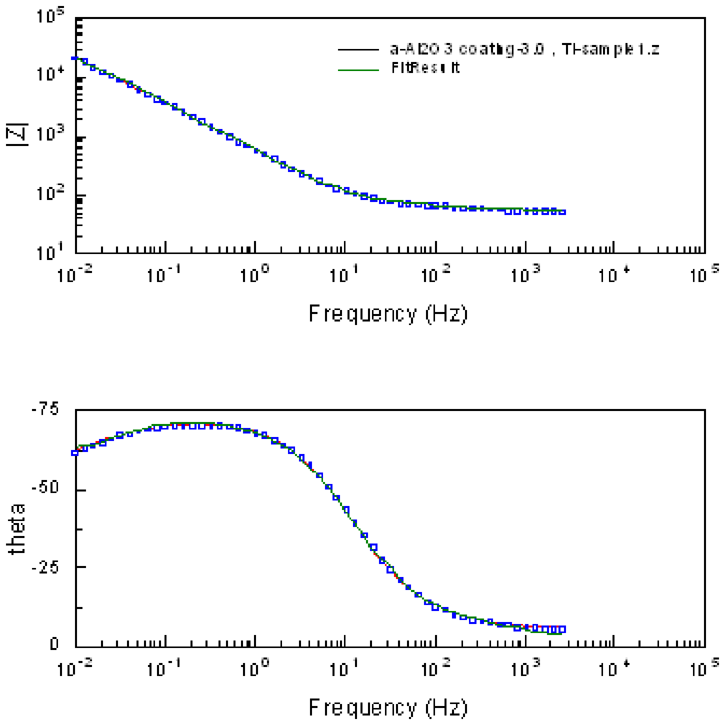

Figure 5: **Impedance spectra recorded for α-alumina coated sample in Hank's solution immediately after exposure.**

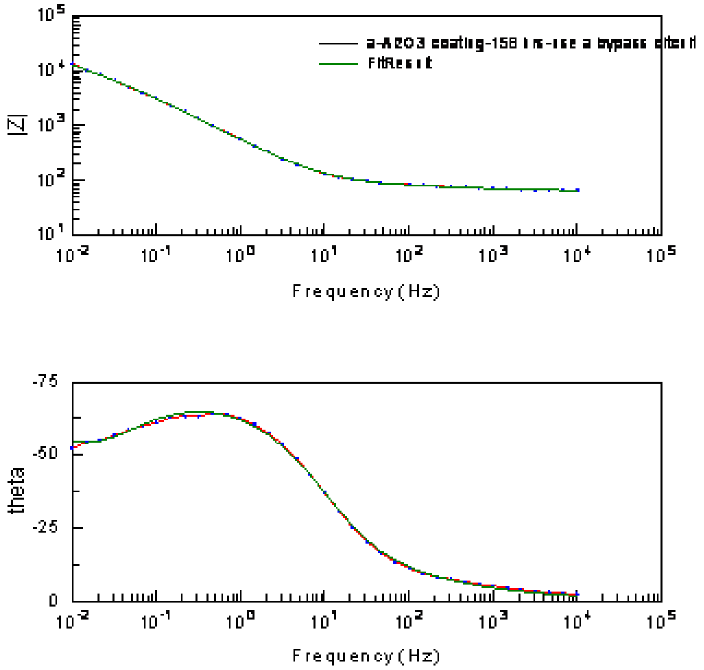

Figure 6: **Impedance spectra recorded for α-alumina coated sample in Hank's solution after 158hrs exposure.**

The plots displayed in Figure 4 exhibit two time constants at longer exposure times. That is, they can be divided into two distinct frequency regions: the time constant in the high-frequency part, which arises from the uncompensated ohmic resistance due to the electrolytic solution and the impedance characteristics resulting from the penetration of the electrolyte through a porous film, and the low-frequency part accounting for the processes taking place at the substrate/electrolyte interface. Such a behavior is observed in metallic materials covered by a porous film, and can be described in terms of an equivalent circuit which accounts for the different electrochemical processes occurring in the system.

For the interpretation of the electrochemical behavior of the system, a physical model of the electrochemical reactions occurring on the electrodes is necessary. The electrochemical cell, because it presents an impedance to a small sinusoidal excitation, may be represented by an equivalent circuit [22, 23]. An equivalent circuit consists of various arrangements of resistances, capacitors, and other circuit elements, and provides the most relevant corrosion parameters applicable to the substrate/electrolyte system. After testing a number of different electrical circuit models in the analysis of the impedance spectra obtained at different exposure times, the appropriate equivalent circuits were obtained. The equivalent circuits consist of the following elements: a solution resistance R_s of the electrolyte, electrical leads, etc., the capacitance C_{pe1} of the coating layer, the charge transfer resistance associated with the penetration of the electrolyte through the pores or pinholes existing in the coating R_1, and the Warburg element W_1 due to the impedance associated with diffusion.

A reasonable fit to the equivalent circuit for a given impedance spectra was established by admitting a relative error of less than 1% for the real and imaginary parts of the impedance.

Next, the quality of fitting was judged by the error distribution versus the frequency comparing experimental with simulated data for different models. Thus, when Ti is exposed to the Hank's solution, its EIS spectra exhibit behavior typical of a film on the metallic substrate. Electrolyte penetration occurs through the pores of the film, thus exposing the underlying metal to the physiological environment. At longer exposure time EIS spectra reflect the fact that the film is changing its characteristics forming a double layer TiO_2. In this case, the double-layer titanium oxide film is hypothesized to consist of a $Ti–TiO_2$ inner-TiO_2 outer porous unsealed layer.

The behavior of samples coated with alumina layer was similar to that of Ti in the beginning except for the Warburg impedance. The Warburg impedance accounts for the Faradic process - namely, the transfer of ions across the coating which is pre-existing in this case. Interestingly, the impedance spectra and the equivalent circuit did not change with time for the case of coated samples. As shown in Figure 7 and 8, the coating morphology after 158 hours (Figure 7) was virtually unchanged from the original form (Figure 8). This indicates that the alumina layer is a stable passive layer.

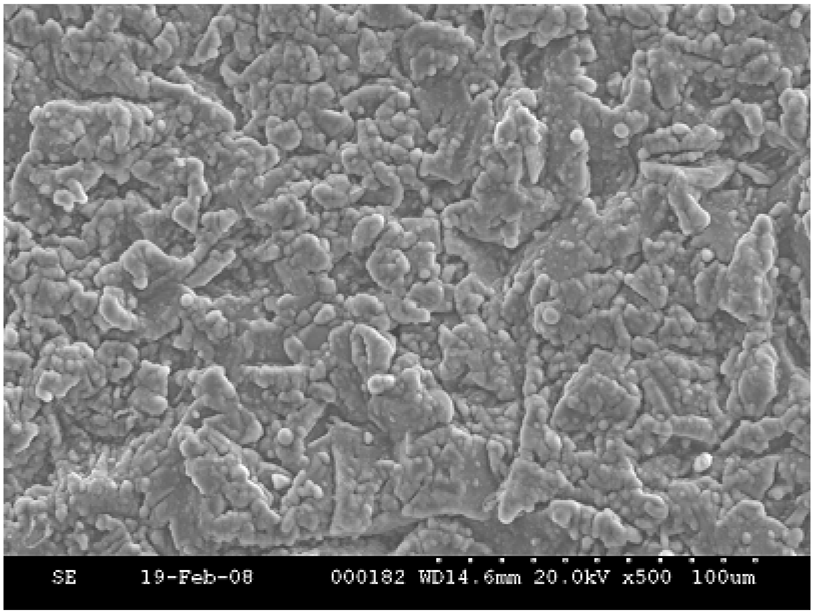

Figure 7: **α-Al2O3 coating sample after 158hrs exposure to Hank's solution**

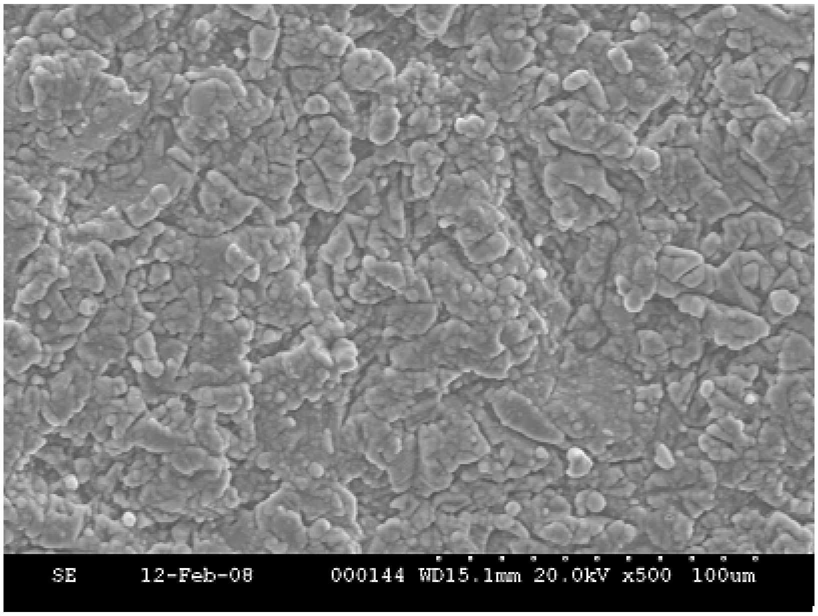

Figure 8: **An SEM view of the surface of a coated alumina film prior to corrosion test.**

The friction characteristics of the coating as well as the base material are shown in Figure 9. Contrary to the expectation, the friction coefficient of the coating tends to be higher than the uncoated sample. The reasons for the rougher than expected films is currently being investigated.

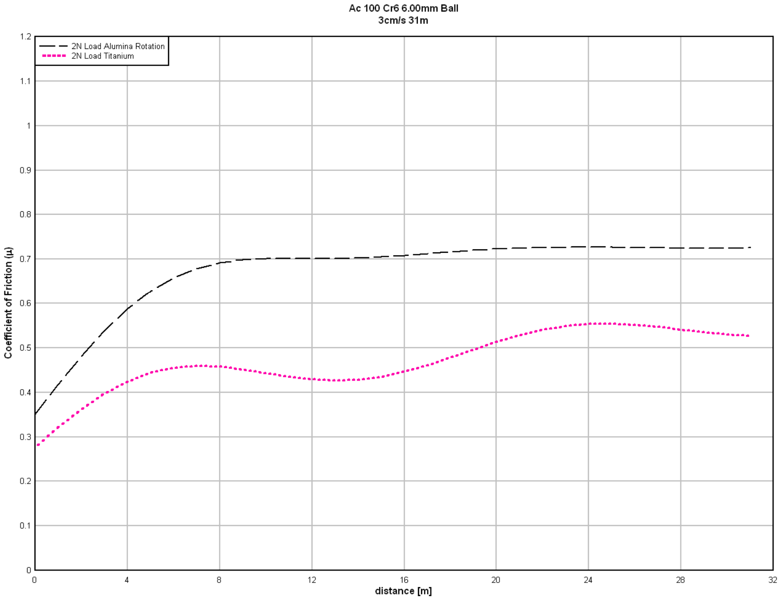

Figure 9: **Friction coefficients of coated and uncoated titanium samples.**

IV. Conclusions

Approximately 750 nm of alumina was deposited on titanium samples using unbalanced magnetron sputtering. TEM results indicate a film of mixed phase with an alpha dominance. Corrosion resistance of the alumina films was significantly better than the uncoated titanium samples. Further, the coated titanium retained its morphology after 158 hours of exposure to a Hank's solution, demonstrating its stability. These data indicate the viability of such a coating for biomedical implants, though the unanticipated increased coefficient of friction needs further study.

Acknowledgments

The authors would like to acknowledge NSF for supporting this work through award #0739659. This work is dedicated to the memory of our colleague, Dr. Deepak G. Bhat.

References

[1] J. Skogsmo, M. Halvarsson, and S. Vuorinen, "Microstructural study of the κ-Al_2O_3→α-Al_2O_3 transformation in CVD κ-Al_2O_3," *Surf Coat. Technol.*, (54-55), 186, 1992

[2] J. E. Sundgren and H. T. G. Hentzell, "A review of the present state of art in hard coatings grown from the vapor phase," *J. Vac. Sci. Technol.*, (4), 2259, 1986

[3] B. Bhushan and B. K. Gupta, *Handbook of Tribology*, McGraw-Hill, New-York, 1991

[4] S. Ruppi, "Deposition, microstructure and properties of texture-controlled CVD α-Al_2O_3 coatings," *Int. J. of Refractory Metals and Hard Materials*, (23), 306, 2005

[5] J. M. Andersson, Zs. Czigany, P. Jinm, and U. Helmersson, "Microstructure of α-alumina thin films deposited at low temperatures on chromia template layers*," J. Vac. Sci. Technol.*, (22), 117, 2004

[6] U. Leushake, T. Krell, U. Schulz, M. Peters, W. A. Kaysser, and B. H. Rabin, "Microstructure and phase stability of EB-PVD alumina and alumina/zirconia for thermal barrier coating applications," *Surf. Coat. Technol.*, (94-95), 131, 1997

[7] M. Mellali, P. Fauchais, and A. Grimaud, "Influence of substrate roughness and temperature on the adhesion/cohesion of alumina coatings," *Surf.Coat. Technol.*, (81), 275, 1996.

[8] J. R. Sobiecki, J. Ewertowshi, T. Babul, and T. Wierzchon, "Properties of alumina coatings produced by gas-detonation method," *Surf. Coat.Technol.*, (180-181), 556, 2004

[9] Y. Chen, X. Ai, C. Huang, and B. Wang, "Preparation of α-alumina coated carbide tools by the sol-gel process," *Mat. Sci. Eng.*, (A 288), 19, 2000

[10] J. Gottmann and E. W. Kreutz, "Functional and structural properties of thin electroceramic films by laser radiation," *Surf. Coat. Technol.*, (116-119), 1189, 1999

[11] R. Cremer, M. Witthaut, D. Neuschutz, G. Erkins, T. Leyendecker, and M. Feldhege, "Comparative characterization of alumina coatings deposited by RF, DC and pulsed reactive magnetron sputtering," *Surf. Coat. Technol.*, (120-121), 213, 1999

[12] T. Kohara, H. Tamagaki, Y. Ikari, and H. Fujii, "Deposition of α-Al_2O_3 hard coatings by reactive magnetron sputtering," *Surf. Coat. Technol.*, (185), 166, 2004

[13] A. Belkind, A. Freilich, G. Song, Z. Zhao, R. Scholl, and E. Bixon, "Mid- frequency reactive sputtering of dielectrics: Al_2O_3," *Surf. Coat. Technol.*, (174-175), 88, 2003

[14] P. Jin, S. Nakao, S. X. Wang, and L.M. Wang, *Appl. Phys. Lett.*, 82 (7) (2003) 1024.

[15] Y. Morikawa, T. Satou, and H. Fujii, JP-P2002-53946A.

[16] A. Aryasomayajula, S. Canovic, D. Bhat, M. H. Gordon, M. Halvarsson, "Transmission electron microscopy and X-ray diffraction analysis of alumina coating by alternating current inverted magnetron-sputtering technique," *Thin Solid Films*, (516), 397, 2007

[17] E. Ryshkewitch and D.W. Richerson, *Oxide Ceramics*, General Ceramics, Inc., Academic Press, Inc., Orlando, FL, and Haskell, NJ, 1985

[18] J.I. Onate, "Wear Reduction Effect on Ultra-High-Molecular-Weight Polyethylene by Appliction of Hard Coatings and Ion Implantation on Cobalt Chromium Alloy, as Measured in a Knee Wear Simulation Machine", *Surf. Coat. Tech.*, (142-144), 1056, 2001

[19] R. Lappalainen, "Reduction of Wear in Total Hip Replacement Prostheses by Amorphous Diamond Coatings", *J Biomed. Mater. Res. B App.l Biomater.*, (66(1)), 410, 2003

[20] R. Overholser and B. Smith, US Patent Application 2007/0078521 A1, "Aluminum Oxide Coated Implants and Components", April 5, 2007

[21] A. N. Cloud, A. Aryasomayajula, D. G. Bhat, and M. H. Gordon, "Determining substrate temperature in an AC inverted cylindrical magnetron sputtering PVD system," *Surf. Coat. Technol.*, (202), 1564, 2007

[22] R. Narayanan and S. K. Seshadri, "Synthesis and corrosion of functionally gradient TiO_2 and hydroxyapatite coatings on Ti-6Al-4V," *Materials Chemistry and Physics*, (106), 406, 2007

[23] J. A. Bardwell and M. C. H. McKubre, "Ac impedance spectroscopy of the anodic film on zirconium in neutral solution," *Electrochim Acta*, (36), 647, 1991

Paper IV: **"Protein Adsorption on Low Temperature Alpha Alumina Films for Surgical Instruments"**
A.N. Cloud, S. Kumar, M. Kavdia, H.H. Abu-Safe, and M.H. Gordon
Submitted to the International Conference on Metallurgical Coatings and Thin Films, Under Review

Protein Adsorption on Low Temperature Alpha Alumina Films for Surgical Instruments

A. N. Cloud, University of Arkansas, Fayetteville, AR 72701, USA
S. Kumar, Ian Wark Research Institute, University of South Australia, Mawson Lakes, Adelaide, SA 5095, Australia
M. Kavdia, University of Arkansas, Fayetteville, AR 72701, USA
H. H. Abu-Safe, University of Arkansas, Fayetteville, AR 72701, USA
M. H. Gordon, University of Arkansas, Fayetteville, AR 72701, USA

Abstract

Bulk alumina has been shown to exhibit reduced protein adsorption, a property that can be exploited for developing alumina-coated surgical instruments and devices. Alpha alumina thin films were deposited on surgical stainless steel substrates to investigate the adsorption of a model protein (BSA, bovine serum albumin). The films were deposited at 480°C by AC inverted cylindrical magnetron sputtering. Films were obtained at 6 kW and 50% oxygen partial pressure by volume. The presence of alpha phase alumina has been shown by transmission electron microscopy. Results indicate that there was a 50% reduction in protein adsorption for samples with the alumina coating compared to those with no coating.

I. Introduction

While the material properties of alpha-phase aluminum oxide have been studied extensively, little is known about the protein adsorption characteristics of alumina thin films. Alumina is a biomedical material that is generally classified as bioinert and has been used for implants and prostheses for several decades [1]. In view of its high hardness (24 GPa) [2], resistance to abrasive wear [2], stability at temperatures upward of 1000°C [3], and biocompatibility, thin alumina coatings are a promising material of choice for value-added applications in the biomedical implant and surgical instrument industries. Alumina-coated stainless steel blades are expected to retain a sharpened edge longer when subjected to hard tissue cutting applications, and the corrosion of alumina-coated stainless steel bone implants can be significantly reduced *in vivo*, resulting in lengthened service lives.

Aluminum oxide is commonly found in nature with an amorphous structure or an array of metastable crystallographic phases (γ, η, θ, δ, and κ). The thermodynamically stable alpha-phase has a hexagonal rhombohedral crystal structure and is the most desirable variant of alumina for intensive wear applications.

Compared to polymeric biomedical materials such as silicones and some metals and alloys, bulk alumina has been shown to exhibit reduced (low and partial surface coverage) protein adsorption [4, 5]. In addition, alumina is expected to be a thromboresistant material [6]. These unique characteristics can be exploited for developing alumina-coated surgical instruments and biomedical devices that are easy to clean to appropriate levels, thus making the otherwise single-use devices reusable. The surfaces of these instruments and devices can be coated with alumina by CVD (chemical vapor deposition) or PVD (physical vapor deposition) methods.

The synthesis of alpha alumina by chemical vapor deposition (CVD) has been extensively investigated and replicated in industry [7]. In CVD, however, the temperature of deposition is roughly 1000°C; while this ensures a good bond between the substrate and coating, the thermal expansion mismatch leads to the accumulation of residual stresses that adversely affect the adhesion of the film. In addition, the high deposition temperatures can result in inefficiencies in an industrial setting as more time must be allowed for cooling of the coated substrate.

Physical vapor deposition processes present a suitable alternative to CVD while alleviating some of the problems associated with high deposition temperatures. PVD techniques typically include electron beam evaporation, plasma spraying, gas detonation, laser ablation, RF sputtering, DC- and pulsed DC magnetron sputtering, and mid-frequency AC magnetron sputtering. Each of these techniques has been used to deposit amorphous alumina coatings that were subsequently converted to an alpha-phase during post-deposition heat treatment at temperatures in excess of 750°C [8-15].

An alternative approach is to promote the growth of alpha alumina using an alpha-phase chromium oxide template layer. Andersson *et al.* [16], Jin *et al.* [17], Morikawa *et al.* [18], and Aryasomayajula *et al.* [19] have independently reported that alpha alumina could be deposited using a chromium oxide template layer. Alpha alumina and alpha-phase chromium oxide are isostructural [3]; the deposition of alpha-alumina is facilitated by the presence of the chromia layer [20]. In the recent past we have succeeded in producing alpha-alumina coatings at a deposition rate of ~125 nm/h [19] with substrate temperatures during deposition shown to be approximately 480°C [21].

Surfaces coated with an alumina film are expected to be more easily cleaned by conventional hospital cleaning methods, compared to uncoated ones, and remain relatively scratch-free due to their high hardness and wear resistance. The residual (protein) bioburden after cleaning is also expected to be significantly reduced, a feature highly desirable for reducing costs in the health care industry through reuse of adequately cleaned otherwise single-use devices and instruments. The reduction of surface scratching is expected to mitigate bio-soiling despite repeated operation cycles. For the work presented and discussed in this paper, protein adsorption studies on alpha alumina-coated surgical stainless steel substrates using a model protein (BSA, bovine serum albumin) have been conducted and compared to studies of an uncoated control.

II. Experimental

Thin films of aluminum oxide were deposited on stainless steel surgical blades using an Isoflux ICM-10 dual target AC inverted cylindrical unbalanced magnetron sputtering system. Two aluminum targets (99.99% purity) act in concert as alternating anode and cathode. High-purity oxygen is supplied to the chamber and allowed to react with the sputtered aluminum to form the alumina coating. The plasma is sustained with an argon working gas. The Ar/O_2 ratio is 1:1.

The deposition chamber is approximately 35 cm in diameter and provides roughly 30 cm of deposition space in the vertical direction. The magnetron is powered by an Advanced Energy PE-II alternating current power supply operating at 40 kHz; substrate biasing is supplied by an Advanced Energy MDX DC power supply.

The surgical steel blades are of the #10 design and are stainless steel. Prior to deposition the blades were cleaned in an ultrasonic bath of acetone for 20 minutes. Samples were then rinsed with acetone, dried, and blown free of debris with compressed nitrogen before being placed under vacuum in the deposition chamber. Base pressures of $1.5\text{x}10^{-6}$ Torr were attained. Just before deposition substrates are further cleaned by plasma etching using an argon plasma and -80 V of DC biasing.

Half of the samples were given a pre-coating of chromium oxide. Chromium targets of 99.9% purity were sputtered for 15 minutes at 6 kW with an Ar/O_2 ratio of 1:1. The remainder of the samples had no such template layer before alumina deposition.

Aluminum oxide was deposited for a period of 6 hours. Alumina films between 0.5 and 1 micron thickness were desired. The films produced were observed to be on the order of 750 nm thick. To avoid a decrease in deposition rate during the experiment, targets were depoisoned after every hour of deposition *in situ*. A mechanical shutter was raised to place a physical barrier between the substrates and the targets. An argon plasma was used to sputter away the accumulated insulating layer of aluminum oxide that develops on the target during oxide deposition. This process was carried out for 450 seconds; the shutter was then lowered and gas flow rates suitable for oxide synthesis were re-established to continue deposition. The deposition pressure was 2 mTorr. Complete deposition parameters are given in Table I.

Subsequent to deposition, coated substrates were allowed to cool under vacuum until they reached room temperature. This process avoids rapid cooling that may induce film cracking. The films were analyzed using XRD, TEM, SEM, EDS, AFM, and FTIR in reflectance mode.

Fourier transform infrared spectroscopy is a powerful technique for studying protein adsorption onto solid surfaces [22, 23]. Compared to various other techniques used for studying protein adsorption, FTIR has the key advantage that spectra can be obtained quickly and easily in a variety of environments such as in solutions and on solid surfaces of ceramics, metals, and polymers. For protein adsorption studies, coated and uncoated blades were kept in 10 mM BSA solution for one hour. Subsequently, the blades were vacuum dried. A Nicolet 6700 FTIR in reflectance mode was used before and after protein adsorption. FTIR data were collected for wavenumbers between 2000 and 1000 cm^{-1}; resolution was 2 cm^{-1}. A white, titanium dioxide background was used. A KBr beam splitter and DTGS-KBr detector were employed.

III. Results and Discussion

X-ray diffraction studies were used in conjunction with past TEM results on this coating to determine the crystallographic phase. Figure 1 shows the XRD results for an alumina coated blade, a blade coated with chromia and alumina, and a reference sample. Only major peaks are readily visible. The largest peaks at 2θ values of 44.4° and 64.5° degrees are seen in all samples and correspond to the stainless steel blade. In the sample coated only with alumina, a large peak is seen at 38.7 degrees; this is indicative of non-pure alpha-phase alumina. In the sample with a chromia pre-coat, a characteristic peak of alpha-phase chromia is seen at 36.2 degrees. Because the peak for alpha-phase alumina is so close to that of alpha chromia, it can be hidden. Previous TEM work confirms that, near the chromia pre-coat, the alumina is of a mixed phase, though the alpha-phase is dominant [19].

Figures 2(a) and 2(b) show SEM micrographs of the surface of both an uncoated and coated blade, respectively. The presence of the film has a significant impact of the surface texture. Surface roughness values of the uncoated and coated blades were attained using atomic force microscopy, shown in Figures 3(a) and 3(b), respectively. Uncoated stainless steel had a root mean square average roughness of 4.2 nm. Blades coated with an α-Cr_2O_3 / α-Al_2O_3 film had a greatly increased roughness of 58.2 nm. Post-deposition polishing of the alumina films may be required to decrease the coating's roughness, and thus its coefficient of friction, and prevent the accumulation of debris on an instrument's surface. For the purposes of medical implementation, it is undesirable for the chromium oxide used as a template layer to come into contact with the body. Ideally, we will develop a repeatable process to deposit alpha alumina films without the chromia template layer. However, even with the underlying chromia layer, EDS surface studies showed only the presence of aluminum and oxygen. The alumina layer is thought to be sufficiently thick and coherent to prevent exposure of the chromia layer, even given moderate wear, though further study in required.

Figures 4(a) and 4(b) show the FTIR reflection for uncoated and coated blades. The amide I and amide II vibration bands between 1700 and 1500 cm^{-1} are representative of the amide backbone of peptides and proteins. The area under the amide II band centered around 1550 cm^{-1} can be used to quantify the adsorped protein. A linear correlation between the adsorped protein and the area under the amide II band has been demonstrated by Pitt and Cooper [24]. The amide I band centered around 1650 cm^{-1} can be used for extracting structural information of the adsorped protein. The spectra in Figure 4(a) were obtained in order to confirm that there is no overlap between the infrared adsorption bands of the alumina-coated and uncoated substrates and those expected from the adsorped protein (BSA) in the 1500 to 1700 cm^{-1} range.

The FTIR spectra of the coated and uncoated substrates obtained after protein (BSA) adsorption, shown in Figure 4(b), clearly indicate the presence of amide I and amide II bands. The amide I adsorption band in the FTIR spectra of Figure 4(b) is a composite band consisting of at least two primary components centered around 1630 and 1670 cm^{-1} for all the three samples, suggesting the presence of both α-helix and β-sheet conformations of BSA upon adsorption.

Comparing the three samples in Figure 4(b), it is found that the area under the amide II band centered at about 1550 cm^{-1} for the uncoated sample is significantly larger (approximately double) than the alumina coated samples (both with and without chromia pre-coat), suggesting that the alumina coated samples adsorped significantly less protein than the uncoated sample. Multiple FTIR spectra were collected for this study; the results presented are representative of the film's performance. This behavior is in line with that observed for bulk alumina samples. The authors believe that this desirable result, from a bioburden removal perspective, is the first of its kind on magnetron sputtered alumina.

IV. Conclusions

Approximately 750 nm thick alumina films were deposited on stainless steel surgical substrates using unbalanced magnetron sputtering. XRD results indicate a film of mixed phase, though prior TEM work shows the films are mostly alpha phase.

FTIR spectroscopy was used to determine the adsorption of a model BSA protein. Despite increased surface roughness, results indicate a roughly 50% reduced bioburden in those blades coated with an aluminum oxide film.

Future work will further investigate methods of depositing a solely alpha-phase film on surgical instruments, controlling surface roughness, and comparing the wear of coated substrates to conventional surgical implements.

Acknowledgments

The authors would like to acknowledge Dan Ostrowski for his assistance collecting the FTIR spectra. This paper is dedicated to the memory of our colleague, Dr. Deepak G. Bhat.

References

[1] S. F. Hulbert, F. A. Young, R. S. Matthew, J. J. Klawitter, C. D. Talbert, F. H. Stelling, J. Biomed. Mater. Res. 4 (1970) 433.

[2] J. Skogsmo, M. Halvarsson, S. Vuorinen, Surf. Coat. Technol., N/55 (1992) 186.

[3] E. Ryshkewitch, D. W. Richerson, Oxide Ceramics, General Ceramics, Inc., Academic Press, Inc., Orlando, FL, and Haskell, NJ, 1985.

[4] H. Fischer, M. Luk, B. Oedekoven, R. Telle, K. Mottaghy, J. Biomed. Mater. Res., 81A (2007) 982.

[5] A. Rosengren, E. Pavlovic, S. Oscarsson, A. Krajewski, A. Ravaglioli, A. Piancastelli, Biomaterials, 23 (2002) 1237.

[6] Y. Takami, S. Yamane, K. Makinouchi, G. Otsuka, J. Glueck, R. Benkowski, Y. Nose, J. Biomed. Mater. Res., 40 (1998) 24.

[7] S. Ruppi, Int. J. of Refractory Metals and Hard Materials, 23 (2005) 306.

[8] U. Leushake, T. Krell, U. Schulz, M. Peters, W. A. Kaysser, B. H. Rabin, Surf. Coat. Technol., 94-95 (1997) 131.

[9] M. Mellali, P. Fauchais, A. Grimaud, Surf.Coat. Technol., 81 (1996) 275.

[10] J. R. Sobiecki, J. Ewertowshi, T. Babul, T. Wierzchon, Surf. Coat.Technol., 180-181 (2004) 556.

[11] Y. Chen, X. Ai, C. Huang, B. Wang, Mat. Sci. Eng., A 288 (2000) 19.

[12] J. Gottmann, E. W. Kreutz, Surf. Coat. Technol., 116-119 (1999) 1189.

[13] R. Cremer, M. Witthaut, D. Neuschutz, G. Erkins, T. Leyendecker, M. Feldhege, Surf. Coat. Technol., 120-121 (1999) 213.

[14] T. Kohara, H. Tamagaki, Y. Ikari, H. Fujii, Surf. Coat. Technol., 185 (2004) 166.

[15] A. Belkind, A. Freilich, G. Song, Z. Zhao, R. Scholl, E. Bixon, Surf. Coat. Technol., 174-175, (2003), 88.

[16] J. M. Andersson, Z. Czigany, P. Jin, U. Helmersson, J. Vac. Sci. Technol., A 22 117 (2004) 8.

[17] P. Jin, S. Nakao, S. X. Wang, L. M. Wang, Appl. Phys. Lett., 82 (7) (2003) 1024.

[18] Y. Morikawa, T. Satou, H. Fujii, JP-P2002-53946A.

[19] A. Aryasomayajula, S. Canovic, D. Bhat, M.H. Gordon, M. Halvarsson, Thin Solid Films, v516 (2007) 397.

[20] E. W. Bunting, Journal Research Natl. Bur. Standards (U.S) 6, 947 (1931).

[21] A. N. Cloud, A. Aryasomayajula, D. G. Bhat, M. H. Gordon, Surf. Coat. Technol., v202 (2008) 1564.

[22] K. K. Chittur, Biomaterials 19 (1998) 357.

[23] A. M. A. Pistorius, Spectroscopy Europe, 7 (1995) 8.

[24] W. G. Pitt, S. L. Cooper, Protein at Interfaces: Physicochemical and Biochemical Studies, Eds J. L. Brash and T. A. Horbett, Vol. 343, American Chemical Society, Washington, DC, 1987.

Table 2 - Deposition parameters for chromium oxide and aluminum oxide coatings.

Parameter	**Chromium Oxide**	**Aluminum Oxide**
Ar/O_2 Ratio	1:1	1:1
Substrate Biasing (V)	-35	-35
Magnetron Power (W)	6000	6000
Deposition Time	15 minutes	6 hours
Base Pressure (Torr)	1.5×10^{-6}	1.5×10^{-6}
Deposition Pressure (mTorr)	2.0	2.0

List of Figures

Figure 1: X-ray diffraction results for films with and without a chromia template layer with an uncoated control blade for comparison.

Figure 2: SEM micrographs of an uncoated (a) and alumina coated (b) stainless steel surgical blade.

Figure 3: Three dimensional AFM images of an uncoated (a) and alumina coated (b) surgical blade.

Figure 4: FTIR reflectance spectra of the uncoated and alumina-coated stainless steel blade substrates: (a) before protein adsorption, and (b) after protein (BSA) adsorption.

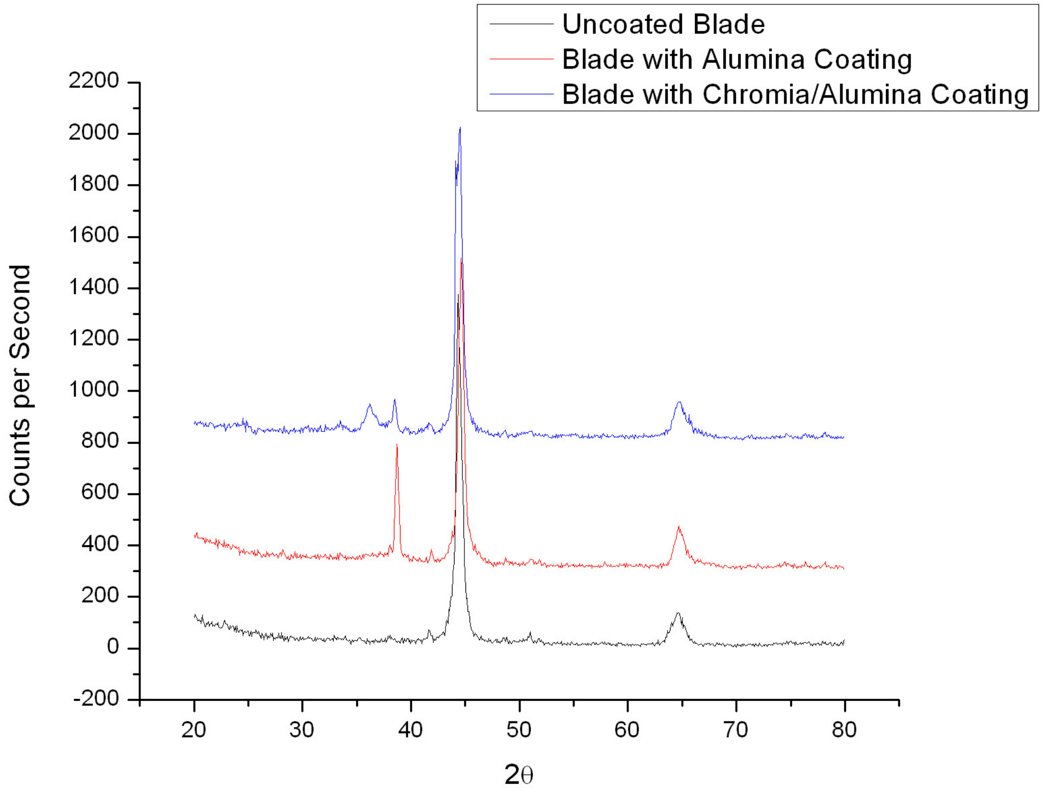
Uncoated Blade
Blade with Alumina Coating
Blade with Chromia/Alumina Coating
Counts per Second
2200
2000
1800
1600
1400
1200
1000
800
600
400
200
0
-200
20
30
40
50
60
70
80
2θ

1

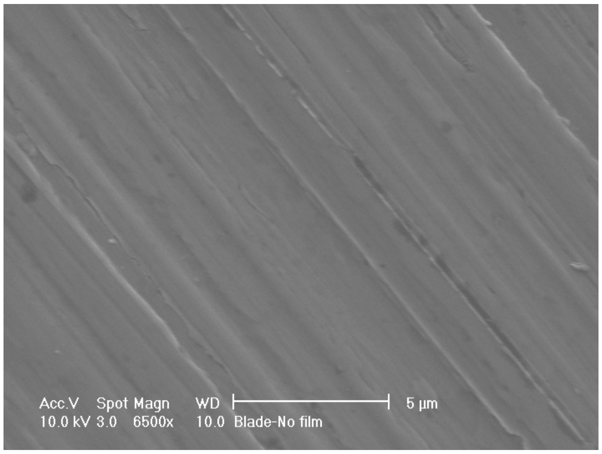
Acc.V Spot Magn WD 5 µm
10.0 kV 3.0 6500x 10.0 Blade-No film

2(a)

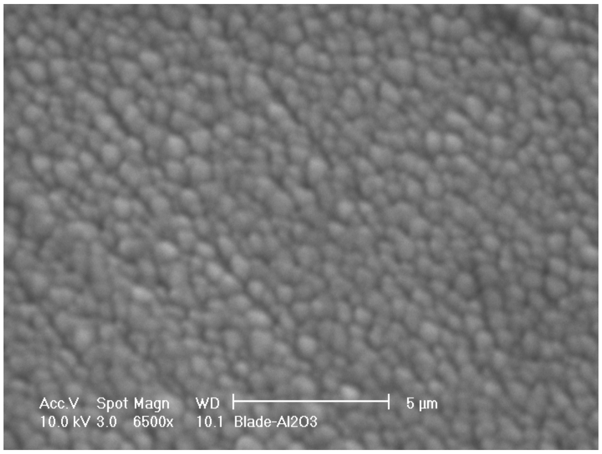
Acc.V Spot Magn WD 5 µm
10.0 kV 3.0 6500x 10.1 Blade-Al2O3

2(b)

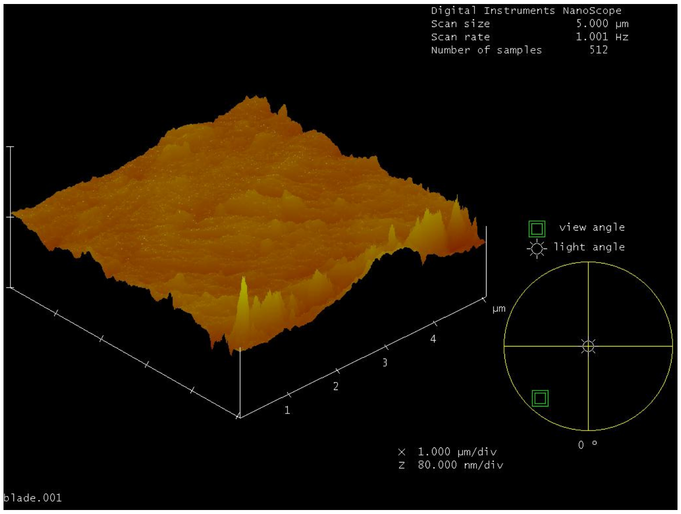
Digital Instruments NanoScope
Scan size 5.000 µm
Scan rate 1.001 Hz
Number of samples 512
view angle
light angle
µm
4
3
2
1
0 °
X 1.000 µm/div
Z 80.000 nm/div
blade.001

3(a)

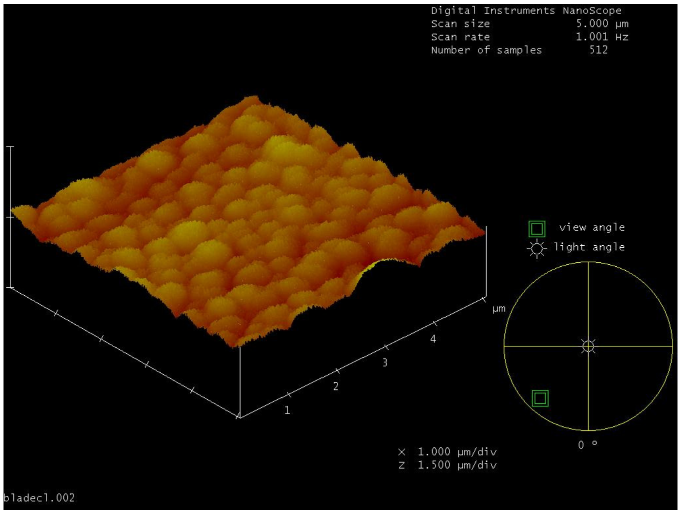
Digital Instruments NanoScope
Scan size 5.000 µm
Scan rate 1.001 Hz
Number of samples 512
view angle
light angle
µm
4
3
2
1
0 °
X 1.000 µm/div
Z 1.500 µm/div
bladecl.002

3(b)

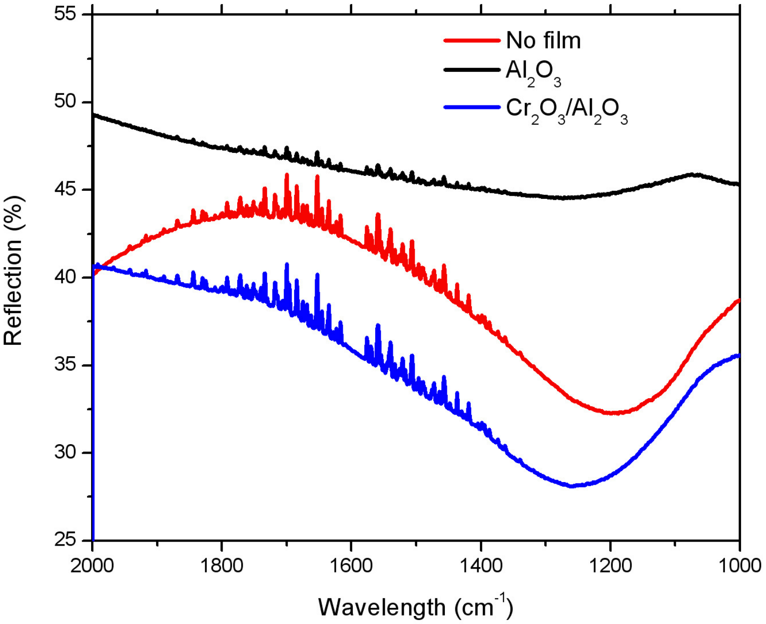

No film
Al_2O_3
Cr_2O_3/Al_2O_3
Reflection (%)
Wavelength (cm^{-1})
55
50
45
40
35
30
25
2000
1800
1600
1400
1200
1000

4(a)

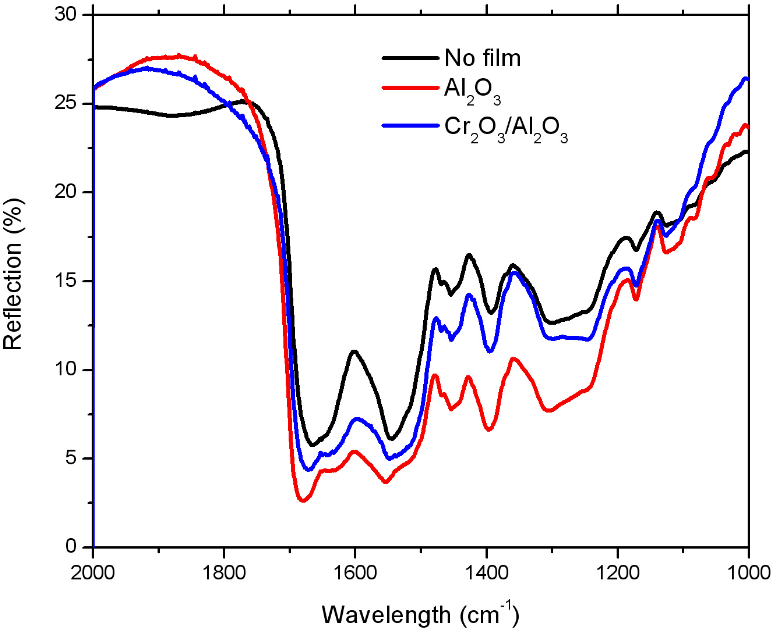

No film
Al_2O_3
Cr_2O_3/Al_2O_3
Reflection (%)
Wavelength (cm^{-1})
30
25
20
15
10
5
0
2000
1800
1600
1400
1200
1000

4(b)

CONCLUSIONS

Alpha-phase aluminum oxide thin films were created using an Isoflux ICM-10 dual target inverted cylindrical magnetron sputtering system using mid-frequency AC power supplies. Alpha alumina films were deposited at a magnetron power of 6 kW, 50% oxygen partial pressure by volume, and -35 V DC bias. Film thickness, substrate material, and position and orientation within the deposition chamber were varied.

The substrate temperatures during deposition were determined experimentally and numerically to be ~480°C at 6kW. TEM studies indicate that the lab's film tend be predominately alpha-phase with discernable gamma-phase components. Corrosion resistance tests indicated that the coated titanium had improved performance and stability compared to the uncoated titanium. However, the coefficient of friction increased with the applied film. There was a 50% reduction in protein adsorption for samples with the alumina coating compared to those with no coating.

The experimental results, in combination with the economics and logistics of the equipment used in the study, are promising for commercialization. The work presented represents only the first steps toward that goal. If progress in this direction continues, the methods described would have an appreciable impact in industry.